What can we learn about axions with PTAs ?

Géraldine SERVANT
DESY/U.Hamburg
Peera Simakachorn
CSIC/U.Valencia

MITP PTA workshop 2023
Mainz, 15-08-2023

CLUSTER OF EXCELLENCE
QUANTUM UNIVERSE

Universität Hamburg

Our Approach .

Rather than interpreting the PTA GW signal in terms of new physics, can we use this measurement to derive constraints on new physics, and in particular, on axion physics?

Which axion physics in the early universe produces GWs at NanoHz frequencies today?

-1- Axionic strings (*= global strings*): this talk

-2- Axion fragmentation

Axions

Among the most hunted particles.

Axions = Pseudo- Nambu Goldstone bosons (PNGBs) from spontaneous breaking of global symmetry which is not exact but broken weakly.

Axion mass is proportional to this breaking.

Very general context.

Historically: QCD axion. Strong dynamics from QCD provides breaking of symmetry.

Axion-like-particles (ALPs): other axions whose mass is not affected by QCD. They get their mass from other sources.

Ubiquitous in many extensions of the Standard Model (in particular in string theory)

Axion-Like-Particles (ALPs).

Consider complex scalar field

$$\Phi = \phi e^{i\theta}$$

charged under anomalous U(1) global symmmetry (Peccei-Quinn symmetry)

Spontaneously broken at scale f_a $V(\varphi) = \lambda \left(|\varphi|^2 - \frac{f_a^2}{2} \right)^2$

$$\langle \boldsymbol{\varphi} \rangle = f_a/\sqrt{2}$$

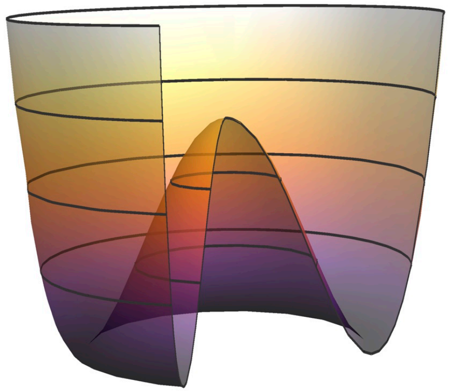

Axion as Goldstone boson

$$\theta \to \theta + \text{const.}$$

$$\boxed{\theta = a / f_a}$$

ALPs.

Non-perturbative effects at energy Λ_b << f_a break the shift symmetry and generate a potential/mass for the axion

$$V = m_a^2(T) f_a^2 \left[1 - \cos(\theta)\right]$$

$$m_a = \Lambda_b^2 / f_a$$

QCD axion

$$m_a^2 f_a^2 \approx (76\ \mathrm{MeV})^4$$

Generic ALP

m_a and f_a : free parameters

The hunt for axions.

Mainly through Axion-photon coupling

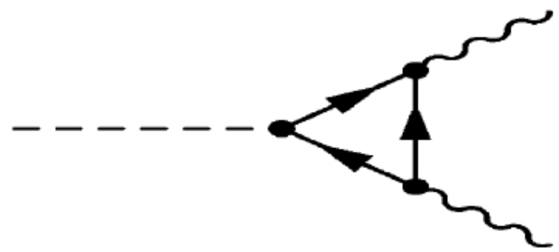

$$\frac{a}{f_a} F_{\mu\nu}\tilde{F}^{\mu\nu}$$

In a background magnetic field:
axion<->photon conversion

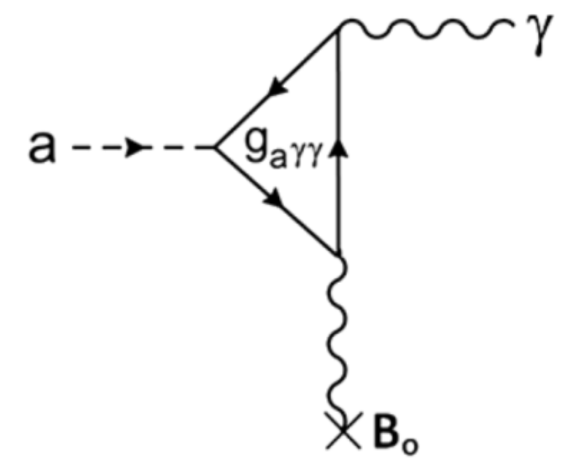

If long-lived: Dark Matter candidate

Three main ways to search for ALPs.

All rely on ALP-photon mixing in magnetic field

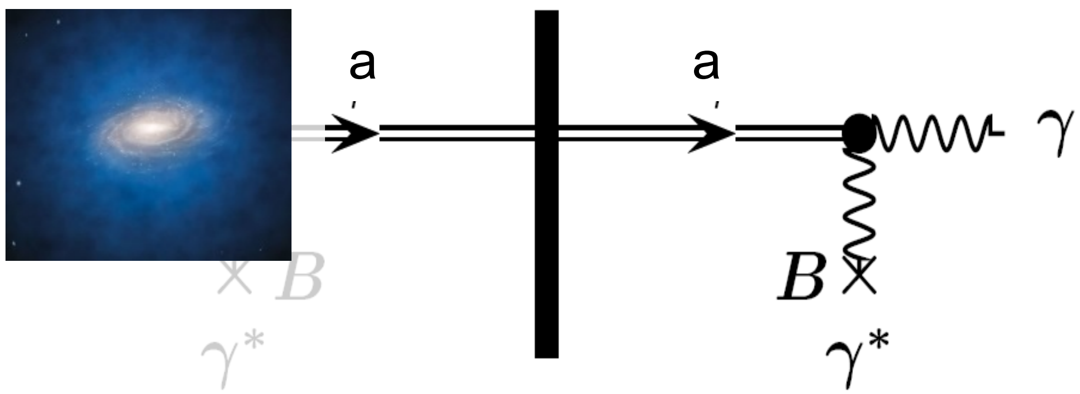

Haloscopes

looking for dark matter constituents, microwaves

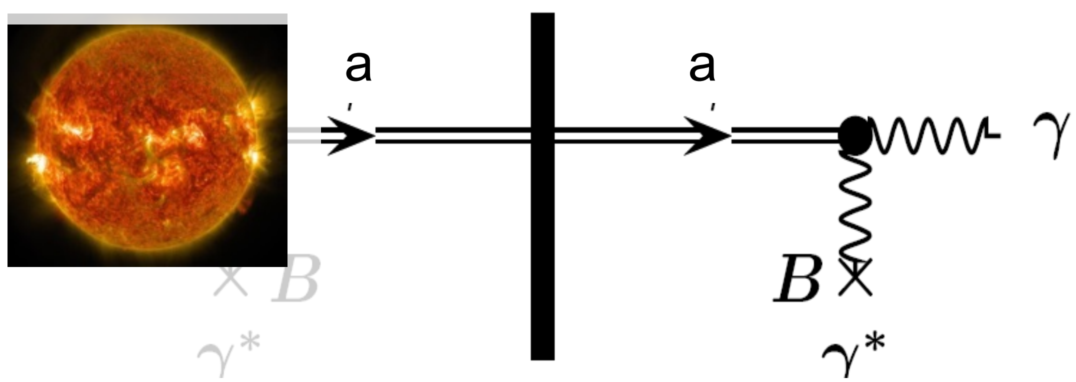

Helioscopes
Axions emitted by the sun, X-rays

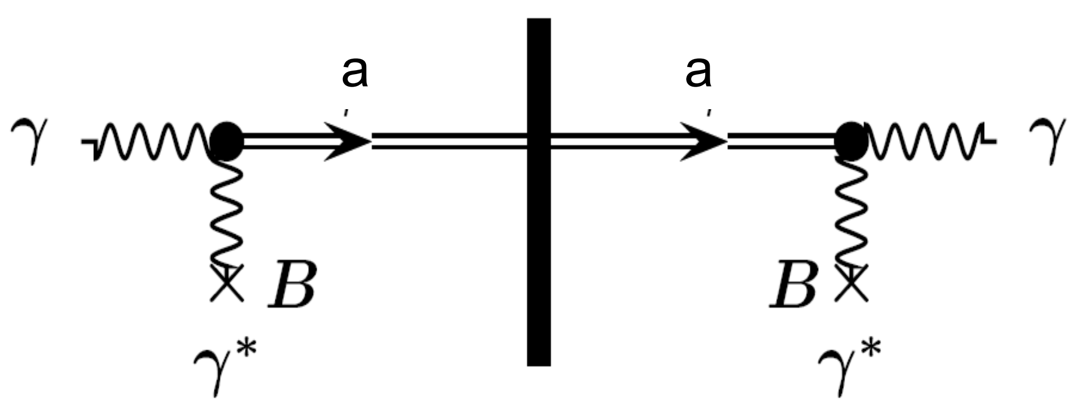

Purely laboratory experiments

“light-shining-through-walls”,

microwaves, optical photons

The Axion-Like-Particle (ALP) parameter space.

If axions are given an interaction to photons then a long list of constraints from ALP searches apply

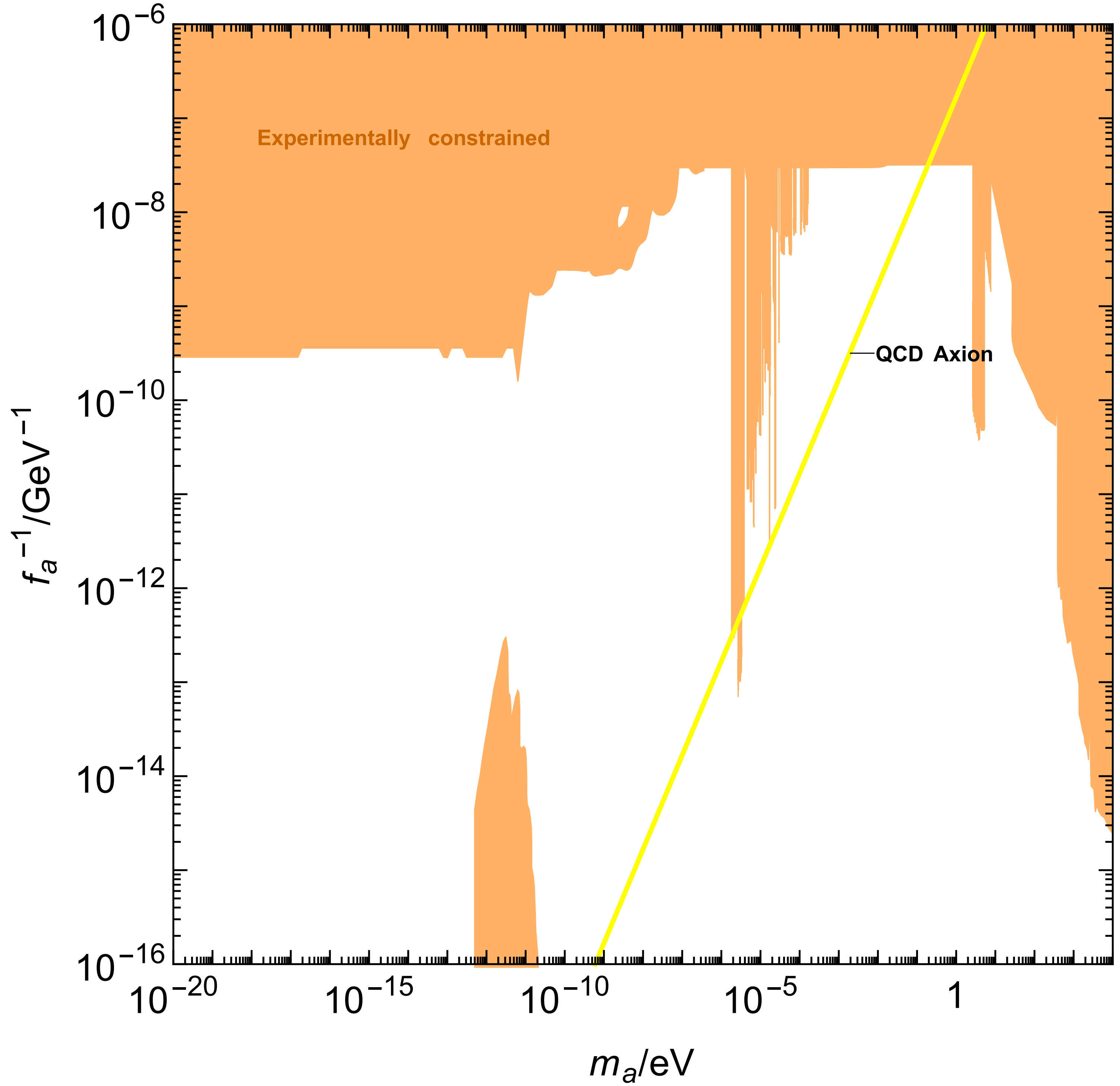

$$\frac{f_\gamma}{f_a} \approx 0.5 \times 10^3$$

assuming KSVZ-like coupling

The hunt for axions.

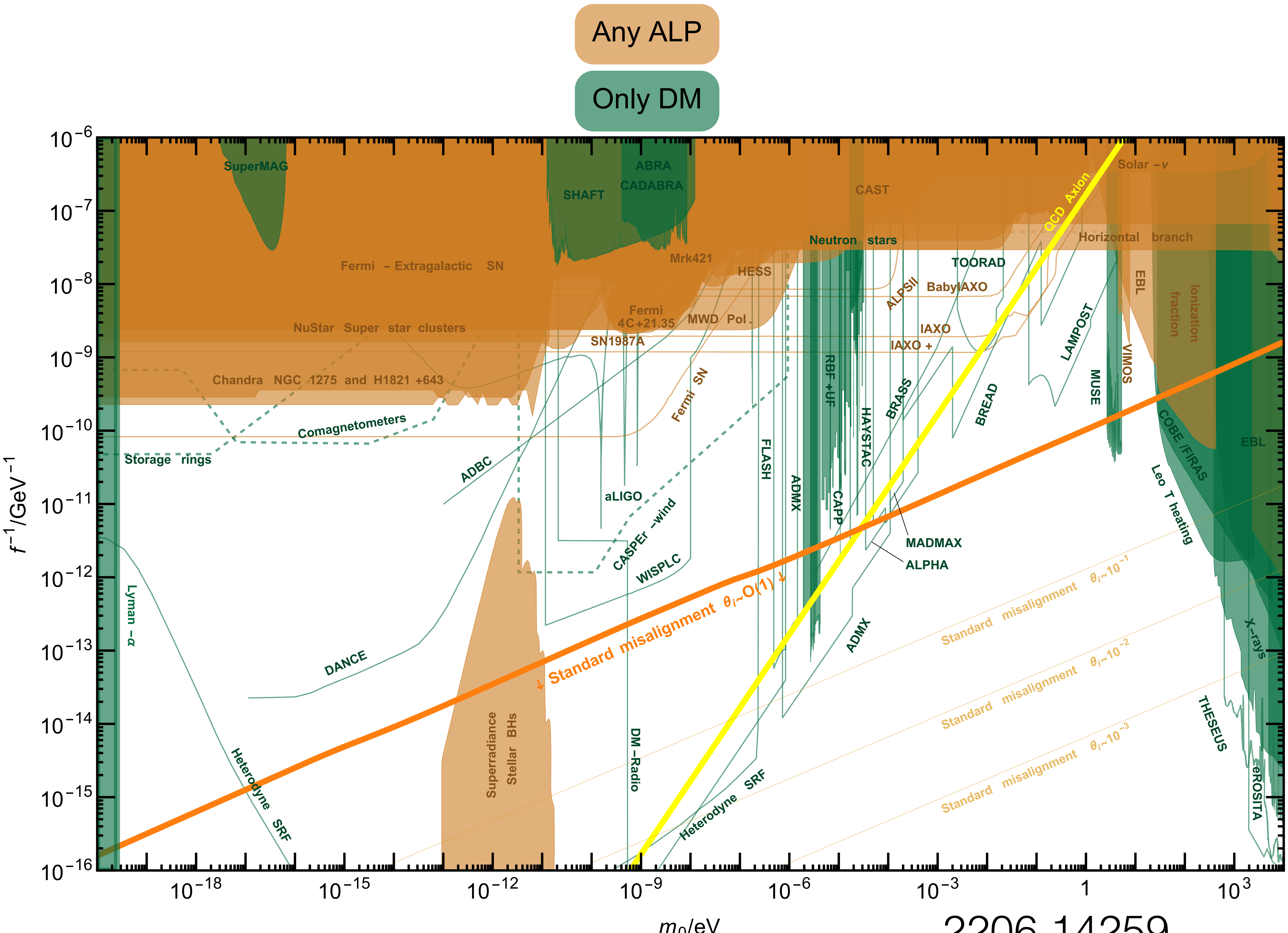

2206.14259

A whole set of experimental constraints.

All data can be found here:

C. O'Hare, *cajohare/axionlimits: Axionlimits*, https://cajohare.github.io/AxionLimits/ (2020) [10.5281/zenodo.3932430].

All experiments also listed in tables 1 and 2 of 2206.14259:

Experiment:	Principle	DM?	Ref.
Haloscope constraints			
ABRACADABRA-10cm	Haloscope	DM	[76]
ADMX	Haloscope	DM	[77–83]
BASE	Haloscope (Cryogenic Penning Trap)	DM	[84]
CAPP	Haloscope	DM	[85–87]
CAST-RADES	Haloscope	DM	[88]
DANCE	Haloscope (Optical cavity polarization)	DM	[89]
Grenoble Haloscope	Haloscope	DM	[90]
HAYSTAC	Haloscope	DM	[91, 92]
ORGAN	Haloscope	DM	[93]
QUAX	Haloscope	DM	[94, 95]
RBF	Haloscope	DM	[96]
SHAFT	Haloscope	DM	[97]
SuperMAG	Haloscope (Using terrestrial magnetic field)	DM	[98]
UF	Haloscope	DM	[99]
Upload	Haloscope	DM	[100]
Haloscope projections			
ABDC	Haloscope	DM	[101]
ADMX	Haloscope	DM	[102]
aLIGO	Haloscope	DM	[103]
ALPHA	Haloscope (Plasma haloscope)	DM	[104]
BRASS	Haloscope	DM	[105]
BREAD	Haloscope (Parabolic reflector)	DM	[106]
DANCE	Haloscope (Optical cavity polarization)	DM	[107]
DMRadio	Haloscope (All stages: 50L, m^3 and GUT)	DM	[108, 109]
FLASH	Haloscope (Formerly KLASH)	DM	[110, 111]
Heterodyne SRF	Haloscope (Superconduct. Resonant Freq.)	DM	[112, 113]
LAMPOST	Haloscope (Dielectric)	DM	[114]
MADMAX	Haloscope (Dielectric)	DM	[115]
ORGAN	Haloscope	DM	[93]
QUAX	Haloscope	DM	[116]
TOORAD	Haloscope (Topological anti-ferromagnets)	DM	[117, 118]
WISPLC	Haloscope (Tunable LC circuit)	DM	[119]
LSW and optics			
ALPS	Light-shining-through wall	Any	[120]
ALPS II	Light-shining-through wall (projection)	Any	[121]
CROWS	Light-shining-through wall (microwave)	Any	[122]
OSQAR	Light-shining-through wall	Any	[123]
PVLAS	Vacuum magnetic birefringence	Any	[124]
Helioscopes			
CAST	Helioscope	Any	[125, 126]
babyIAXO	Helioscope (projection)	Any	[1, 127, 128]
IAXO	Helioscope (projection)	Any	[1, 127, 128]
IAXO+	Helioscope (projection)	Any	[1, 127, 128]

Table 1. List of experimental searches for axions and ALPs. The table is continued in table 2. All experiments here rely on the axion-photon coupling.

Experiment:	Principle	DM?	Reference
Astrophysical constraints			
4C+21.35	Photon-ALP oscillation on the γ-rays from blazars	Any	[129]
Breakthrough Listen	ALP $\to$ radio γ in neutron star magn. fields	DM	[130]
Bullet Cluster	Radio signal from ALP DM decay	DM	[131]
Chandra	AGN X-ray prod. in cosmic magn. field	Any	[132–135]
BBN + $N_{\rm eff}$	ALP thermal relic perturbing BBN and $N_{\rm eff}$	Any	[136]
Chandra MWD	X-rays from Magnetic White Dwarf ALP prod.	Any	[137]
COBE/FIRAS	CMB spectral distortions from DM relic decay	DM	[138]
Distance ladder	ALP $\leftrightarrow \gamma$ perturbing luminosity distances	Any	[139]
Fermi-LAT	SN ALP product. $\to \gamma$-rays in cosmic magn. field	Any	[140–142]
Fermi-LAT	AGN X-ray production $\to$ ALP in cosmic magn. field	Any	[143]
Haystack Telescope	ALP DM decay $\to$ microwave photons	DM	[144]
HAWC TeV Blazars	$\gamma \to$ ALP $\to \gamma$ conversion reducing γ-ray attenuation	Any	[145]
H.E.S.S.	AGN X-ray production $\to$ ALP in cosmic magn. field	Any	[146]
Horizontal branch stars	stellar metabolism and evolution	Any	[147]
LeoT dwarf galaxy	Heating of gas-rich dwarf galaxies by ALP decay	DM	[148]
Magnetic white dwarf pol.	$\gamma \to$ ALP conversion polarizing light from MWD stars	Any	[149]
MUSE	ALP DM decay $\to$ optical photons	DM	[150]
Mrk 421	Blazar γ-ray $\to$ ALP $\to \gamma$-ray in cosmic magn. field	Any	[151]
NuStar	Stellar ALP production $\to \gamma$ in cosmic magn. fields	Any	[152, 153]
NuStar, Super star clusters	Stellar ALP production $\to \gamma$ in cosmic magn. fields	Any	[153]
Solar neutrinos	ALP energy loss $\to$ changes in neutrino production	Any	[154]
SN1987A ALP decay	SN ALP production $\to \gamma$ decay	Any	[155]
SN1987A gamma rays	SN ALP production $\to \gamma$ in cosmic magnetic field	Any	[156, 157]
SN1987A neutrinos	SN ALP luminosity less than neutrino flux	Any	[157, 158]
Thermal relic compilation	Decay and BBN constraints from ALP thermal relic	Any	[159]
VIMOS	Thermal relic ALP decay $\to$ optical photons	Any	[160]
White dwarf mass relation	Stellar ALP production perturbing WD metabolism	Any	[161]
XMM-Newton	Decay of ALP relic	DM	[162]
Astrophysical projections			
eROSITA	X-ray signal from ALP DM decay	DM	[163]
Fermi-LAT	SN ALP production $\to \gamma$ in cosmic magnetic field	Any	[164]
IAXO	Helioscope detection of supernova axions	Any	[165]
THESEUS	ALP DM decay $\to$ x-ray photons	DM	[166]
Neutron coupling:			
CASPEr-wind	NMR from oscillating EDM (projection)	DM	[167, 168]
CASPEr-ZULF-Comag.	NMR from oscillating EDM	DM	[168, 169]
CASPEr-ZULF-Sidechain	NMR (constraint & projection)	DM	[168, 170]
NASDUCK	ALP DM perturbing atomic spins	DM	[171]
nEDM	Spin-precession in ultracold neutrons and Hg	DM	[168, 172]
K-3He	Comagnetometer	DM	[173]
Old comagnetometers	New analysis of old comagnetometers	DM	[174]
Future comagnetometers	Comagnetometers	DM	[174]
SNO	Solar ALP flux from deuterium dissociation	Any	[175]
Proton storage ring	EDM signature from ALP DM	DM	[176]
Neutron Star Cooling	ALP production modifies cooling rate	Any	[177]
SN1987 Cooling	ALP production modifies cooling rate	Any	[178]
Coupling independent:			
Black hole spin	Superradiance for stellar mass black holes	Any	[72–74]
Lyman$-\alpha$	Modification of small-scale structure	DM	[60]

Table 2. List of experimental searches for axions and ALPs.

Do PTAs have anything more to add on this plot ?

Based on
arXiv 2307.03121

with Peera Simakachorn

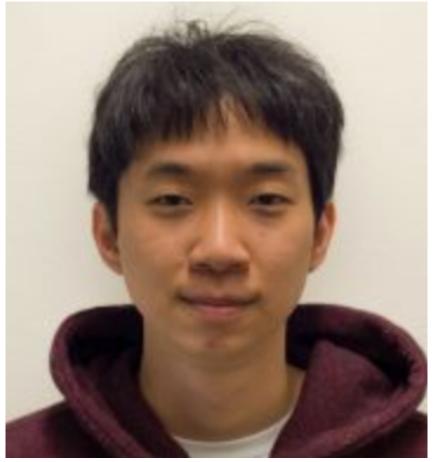

Pre- and post-inflationary scenarios.

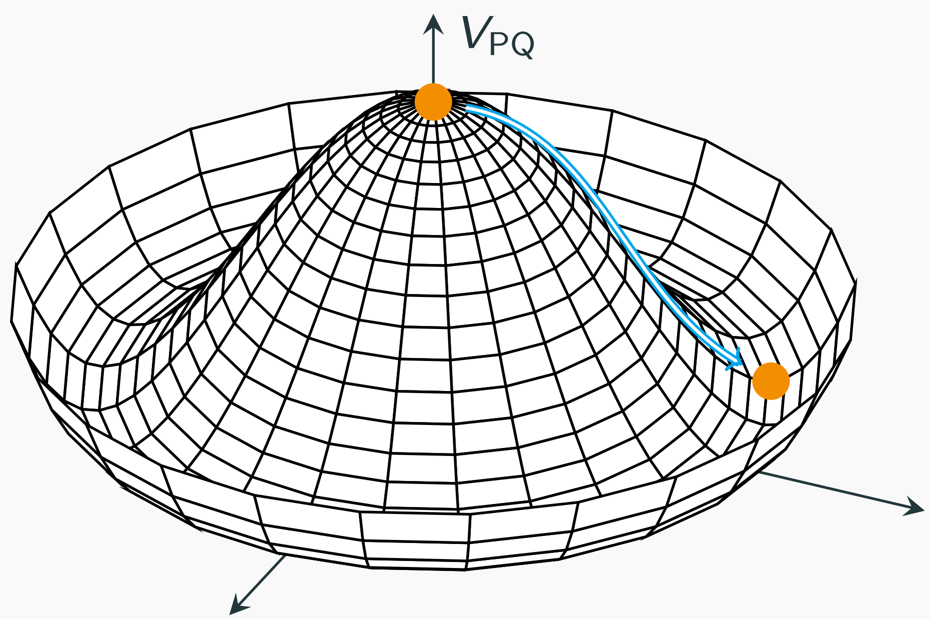

Post-inflationary scenario

- Different initial angle in each Hubble patch.
- Inhomogeneous including topological defects.

GLOBAL (axionic) COSMIC STRINGS

primordial GW bgd

Pre-inflationary scenario

- Random initial angle in the observable universe.
- Initially homogeneous w/o topological defects.

Primordial Gravitational Waves .

Benchmark Primordial Sources of GWs.

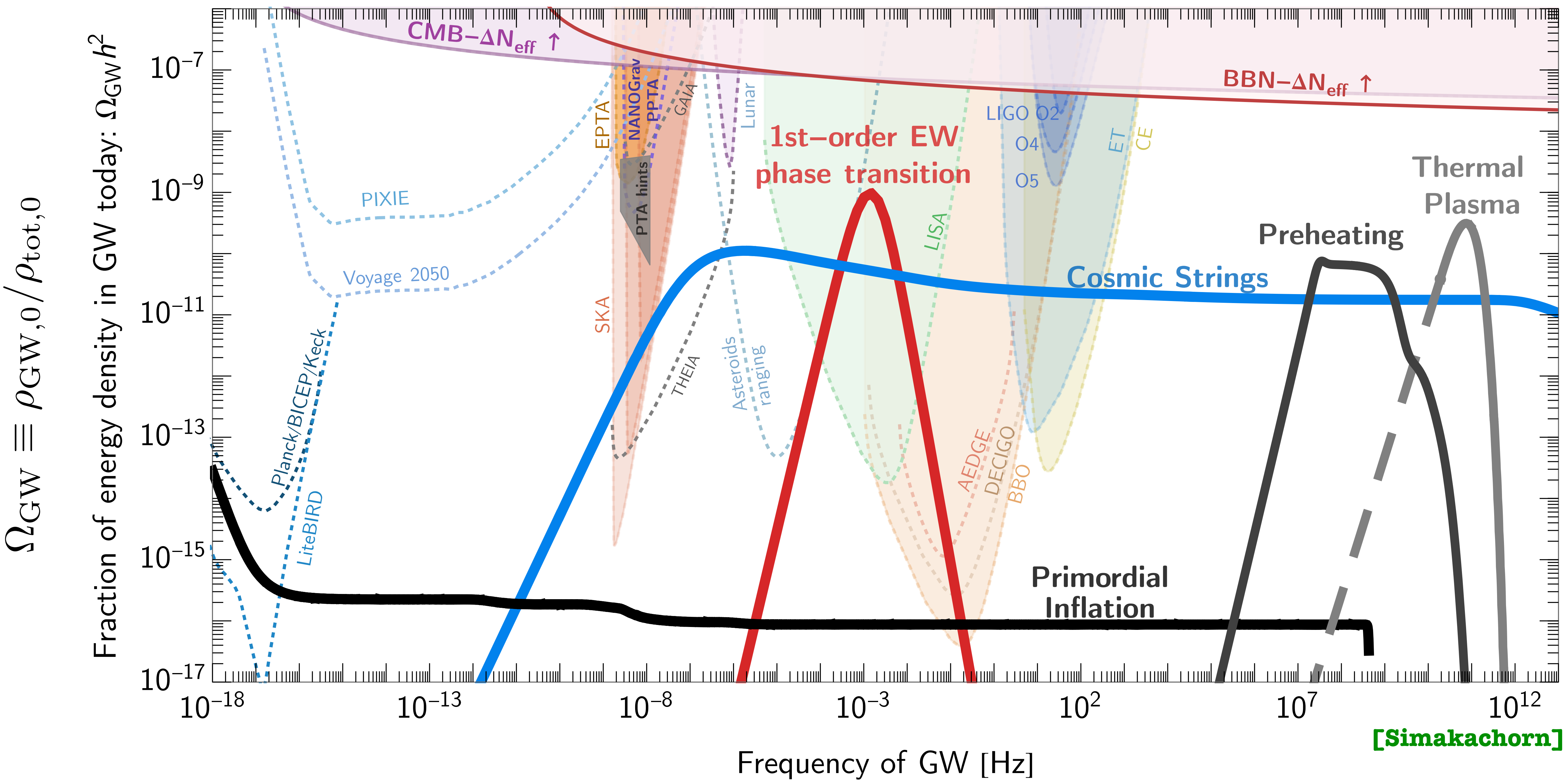

Reading the history of the universe.

GW frequency $f_{\mathrm{GW},0} \simeq \lambda_{\mathrm{GW}}^{-1} \left(\frac{a_{\mathrm{prod}}}{a_0} \right)$

Low-freq. limit

$f_{\mathrm{GW}}^{\min} \simeq H_0^{-1}$
$\simeq 10^{-18}$ Hz

High-freq. limit

$f_{\mathrm{GW}}^{\max} \simeq 10^{13}$ Hz
$(\lambda_{\mathrm{GW}} \sim H^{-1} \sim M_{\mathrm{pl}}^{-1})$

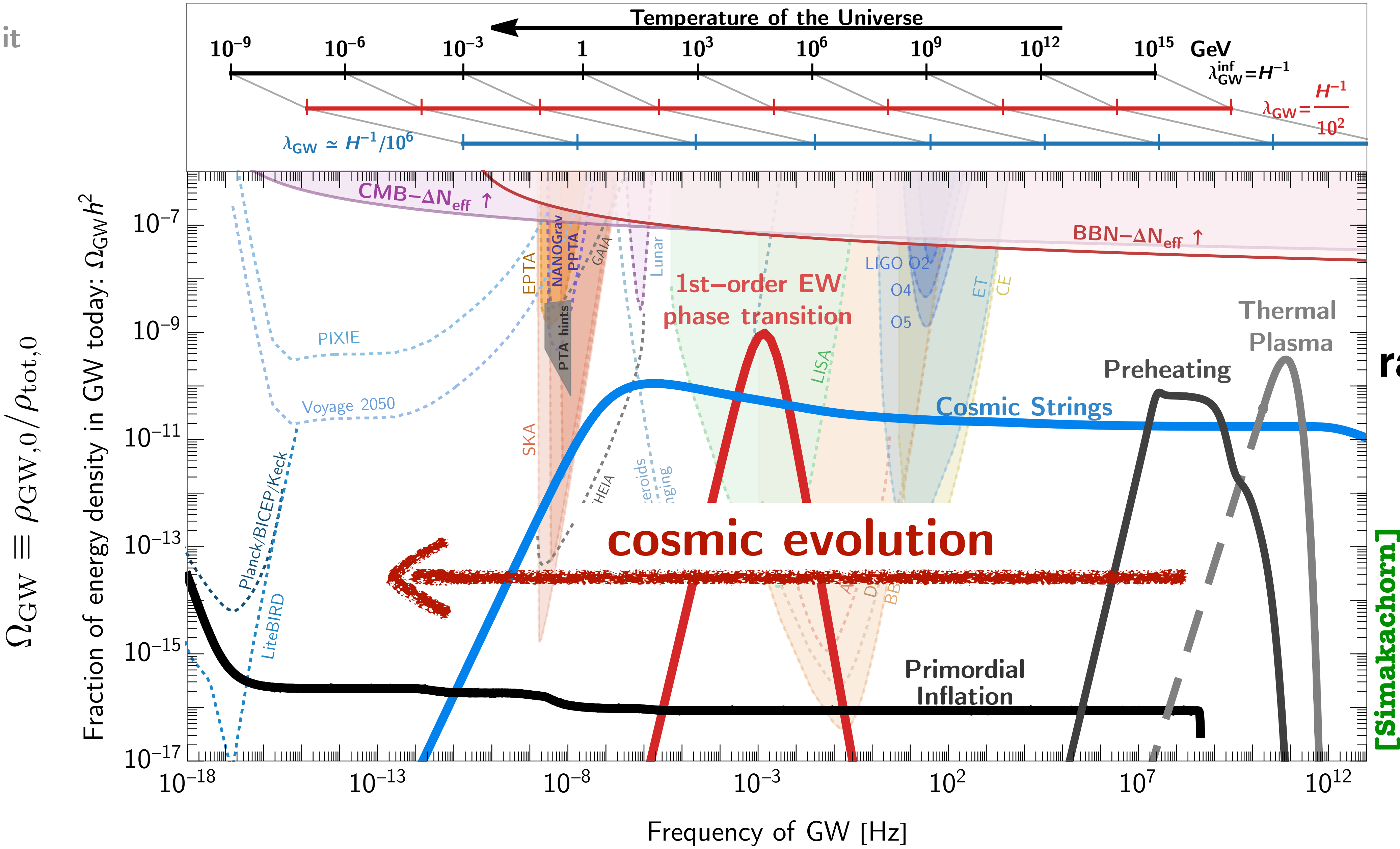

Assuming Standard Model radiation era at high energies

Gravitational Waves from cosmic strings.

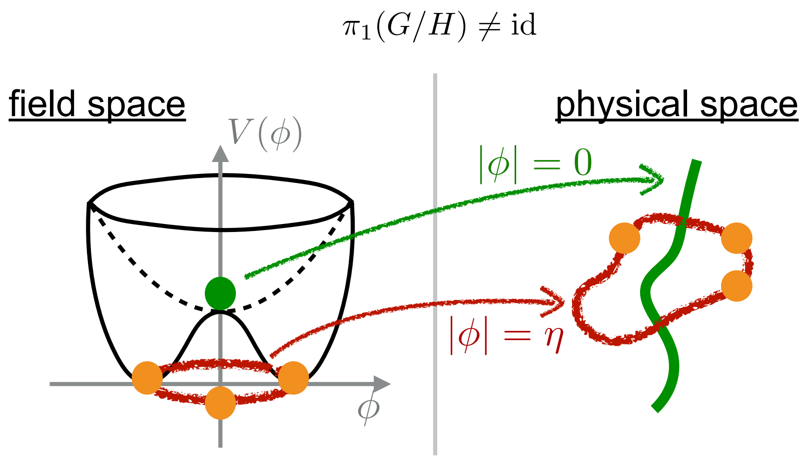

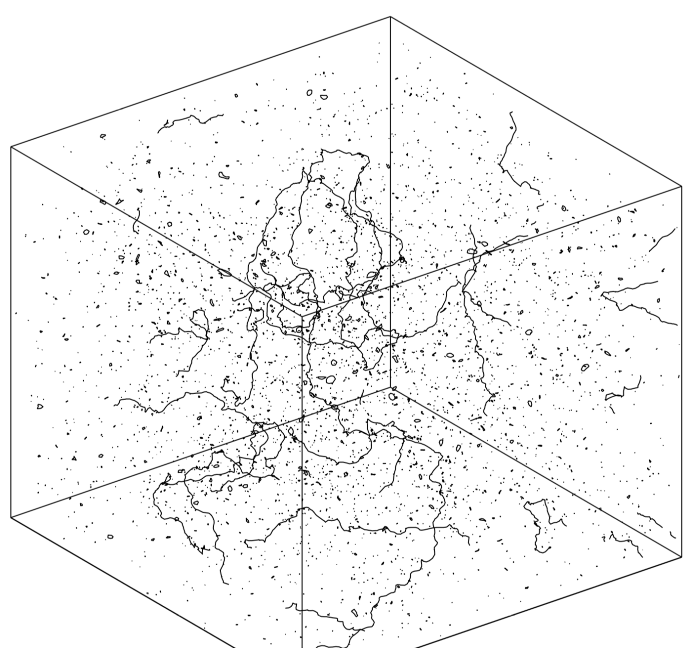

Network of cosmic strings
[Allen & Shellard, 1990]

Cosmic strings:

Long-lasting source of GW

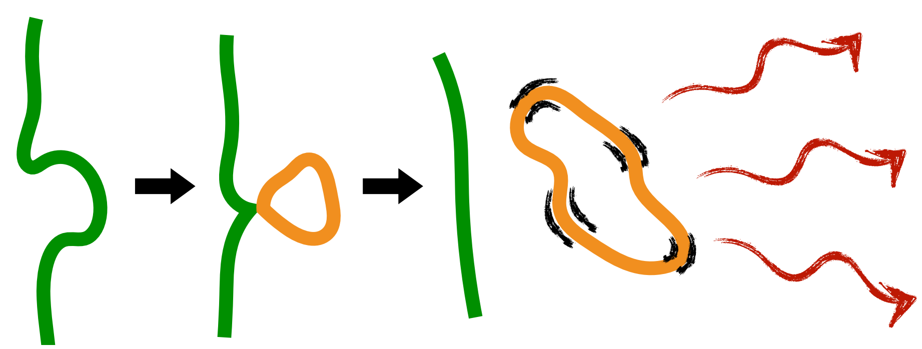

string tension: $\mu \sim \eta^2$

$\eta = f_a$

recent reviews: [1909.00819, 1912.02569]

Loop formation & scaling regime.

String intercommutation: loop formation depletes energy from the network.

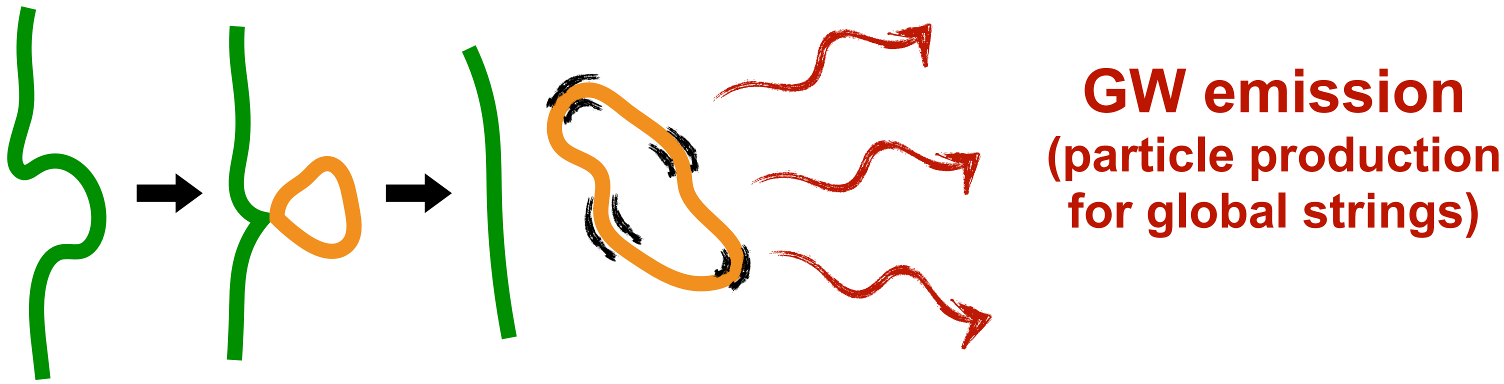

Cosmic strings do not overclose the universe.

Scaling regime:

$$\rho_\infty \propto t^{-2} \propto \begin{cases} a^{-3} & \text{for matter} \\ a^{-4} & \text{for radiation} \\ a^{-6} & \text{for kination} \end{cases}$$

Gravitational Waves from Cosmic strings.

(long-lasting sources).

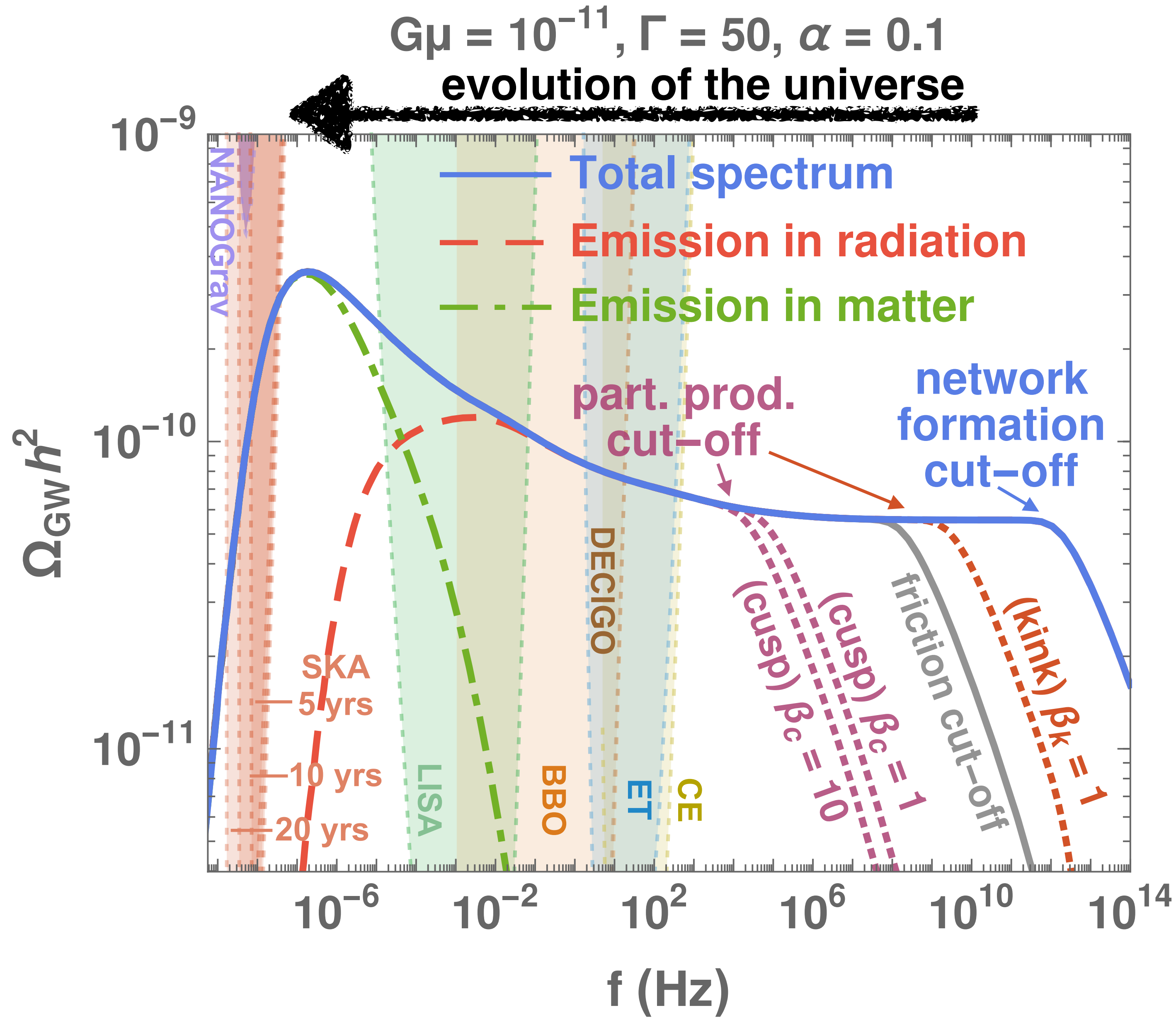

[1912.02569]

Higher f ⇔ Earlier emission

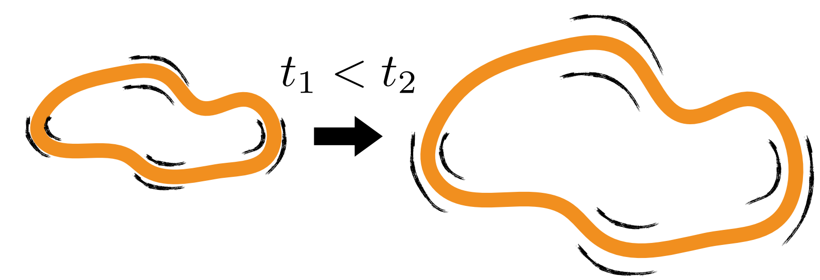

smaller loop ⇔ higher oscillation f

@ earlier t_i

more GW from more loops
but more red-shift

⇨ Flat during radiation

singular structures on loop
(beyond NG approx.)

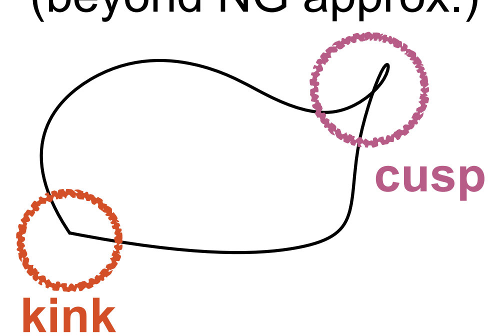

lead to particle emission

Short-lasting vs long-lasting primordial sources.

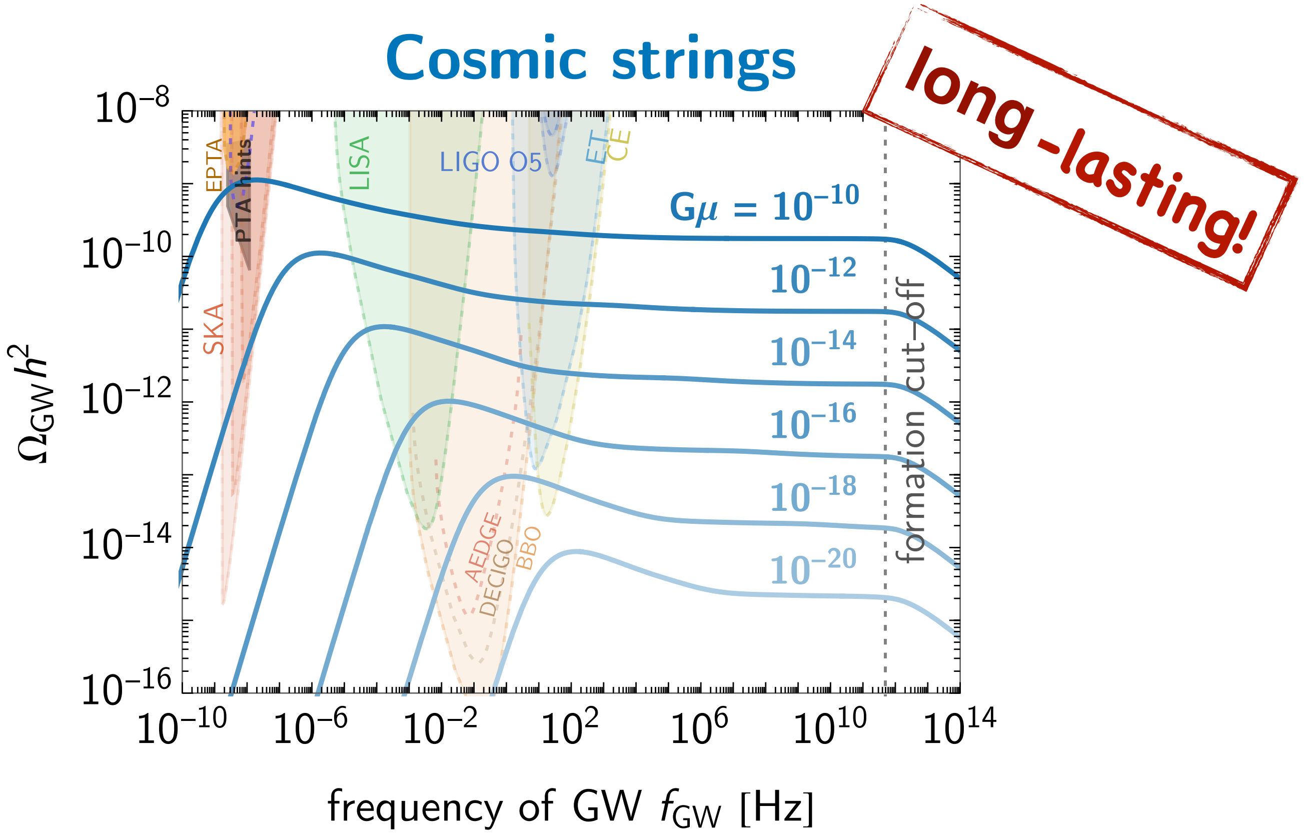

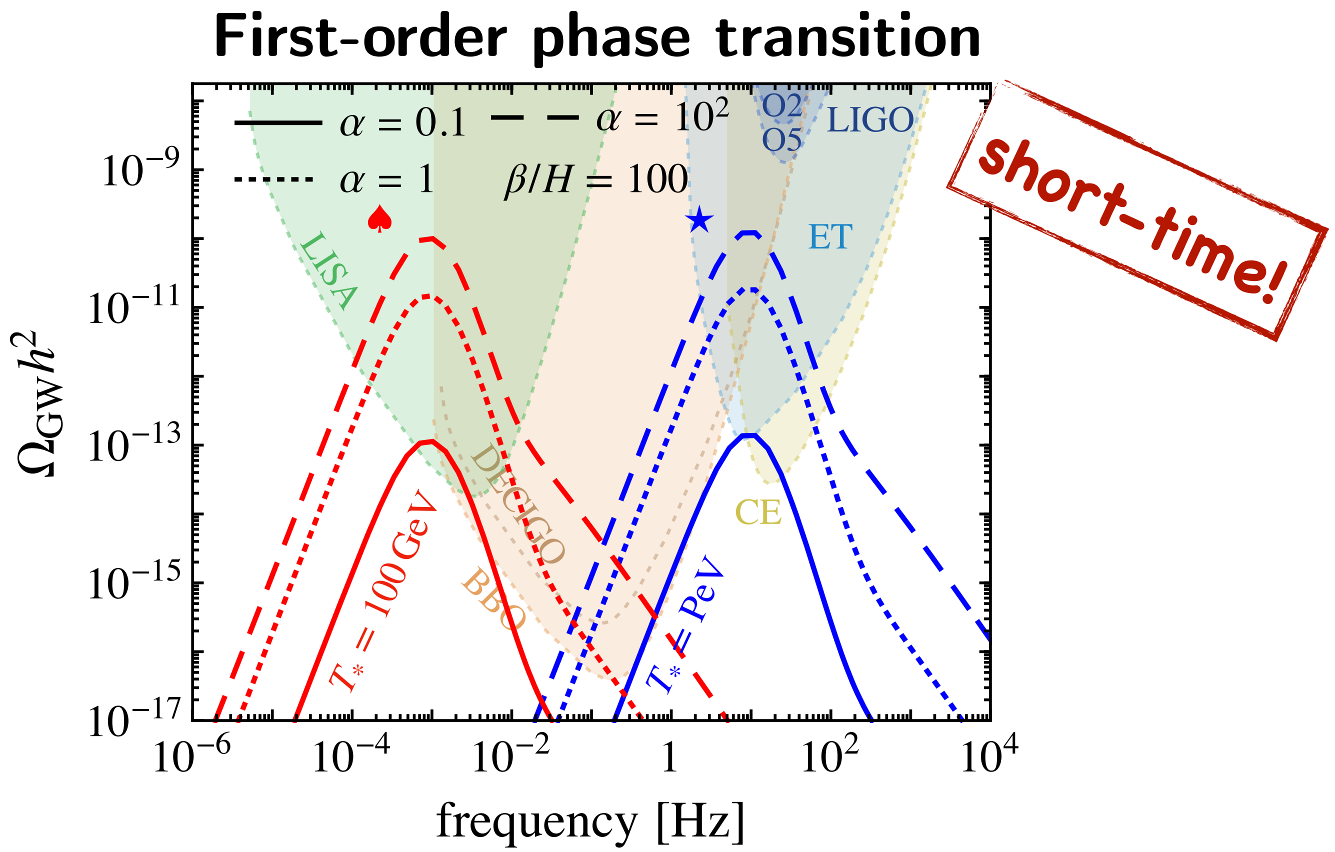

Gravitational Waves from cosmic strings.

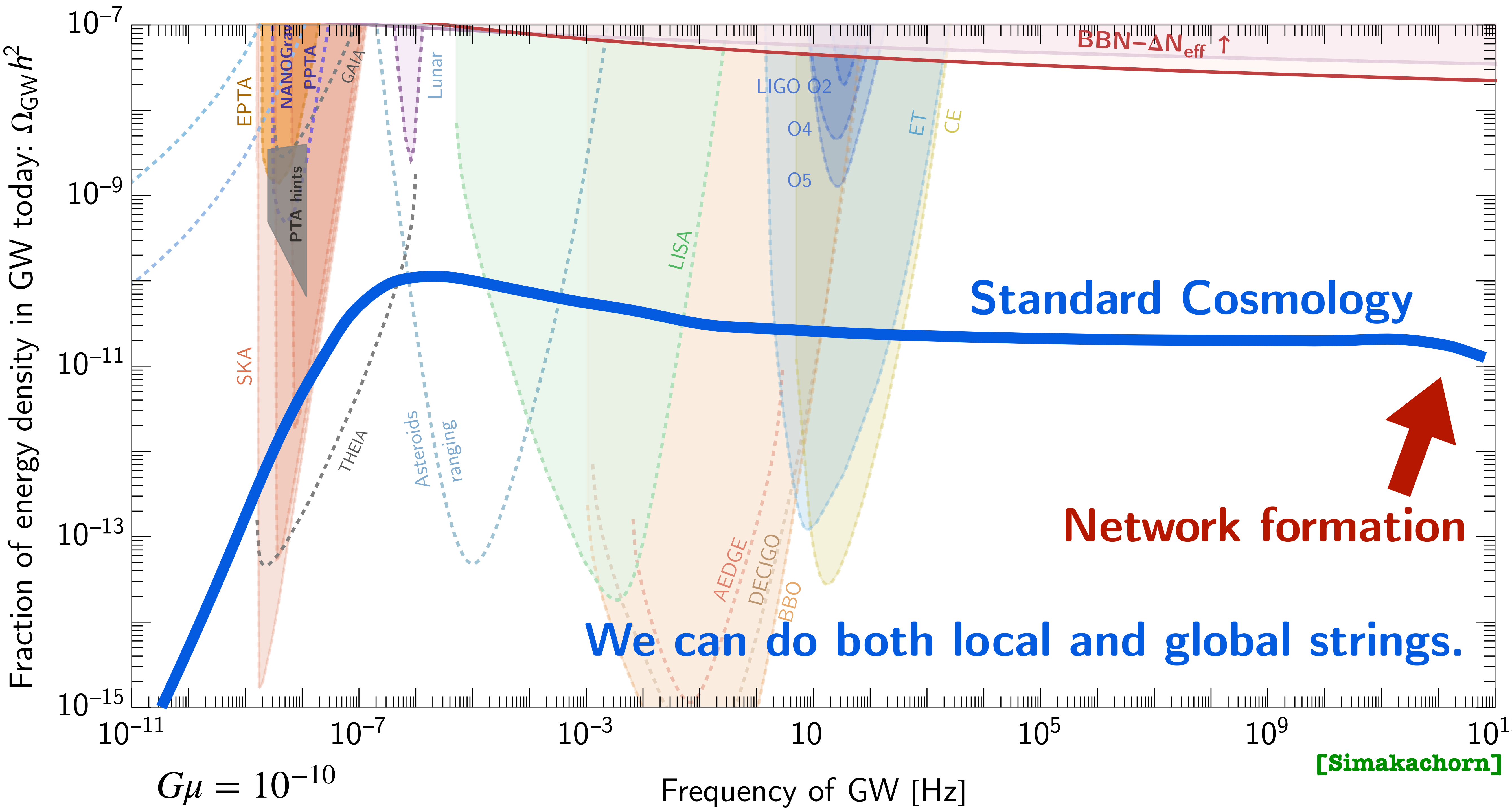

Gravitational Waves from cosmic strings.

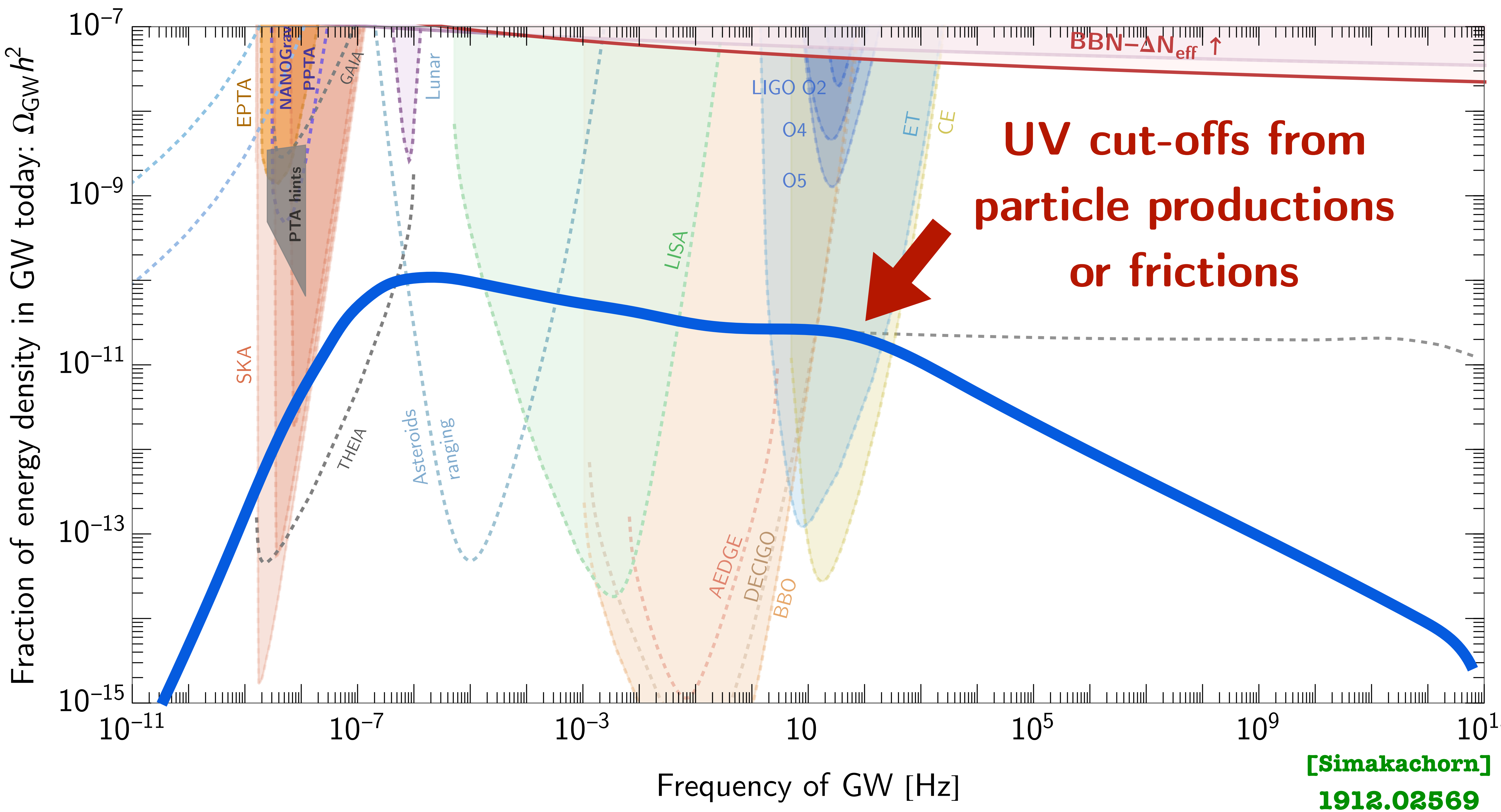

[Simakachorn]
1912.02569

Gravitational Waves from cosmic strings.

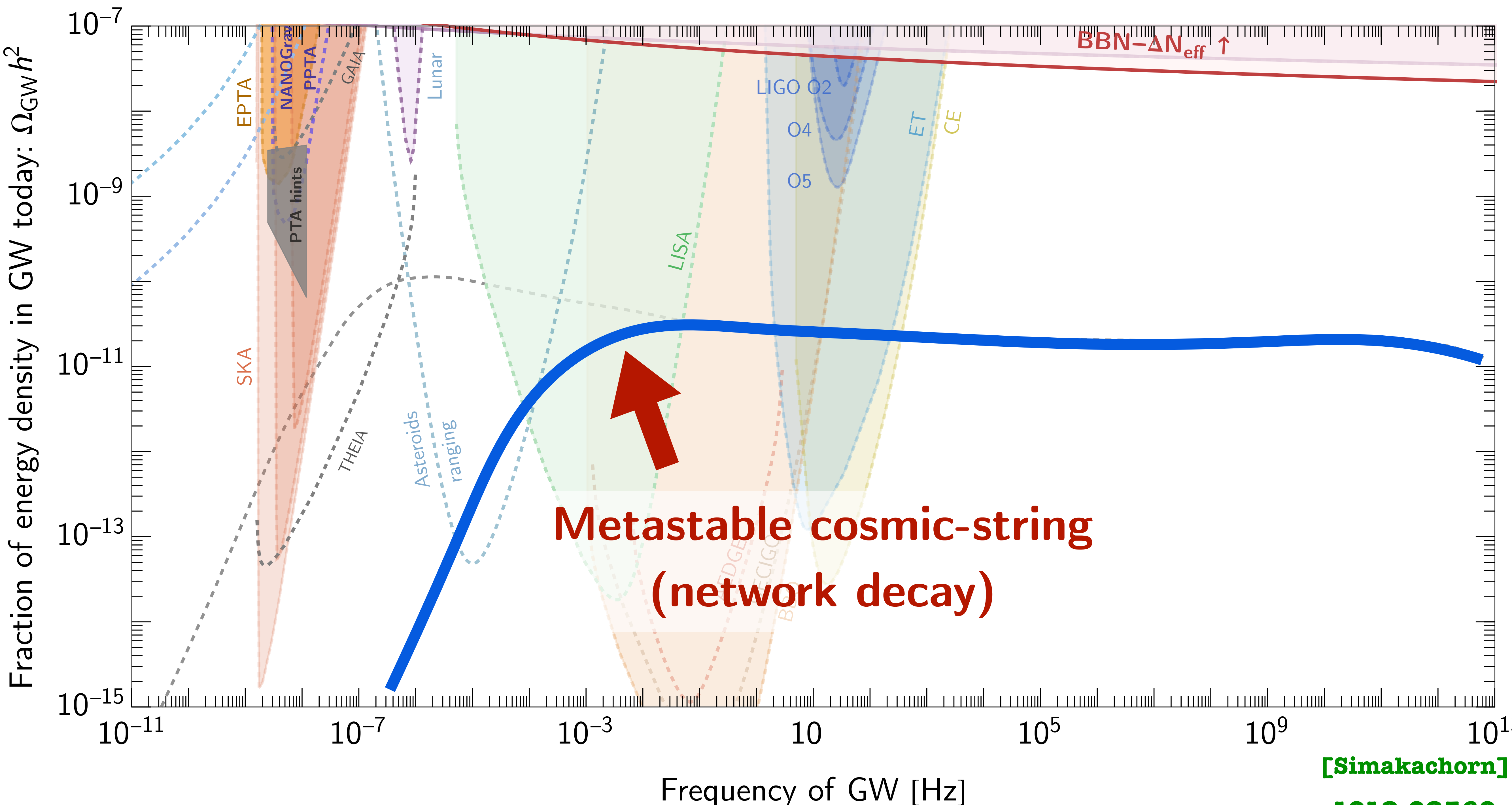

[Simakachorn]

1912.02569

Gravitational Waves from cosmic strings.

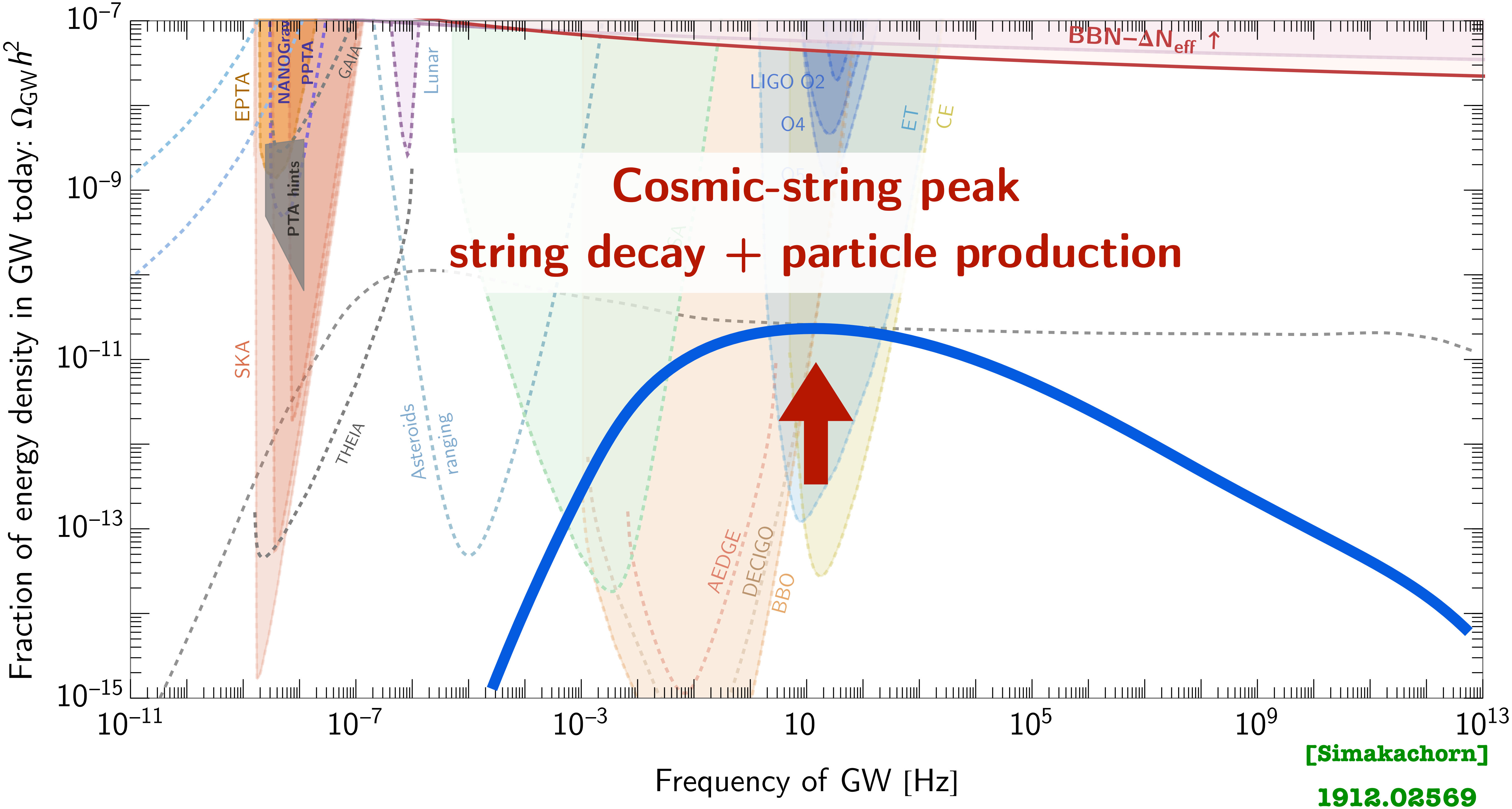

[Simakachorn]

1912.02569

LOCAL STRINGS

vs

GLOBAL STRINGS.

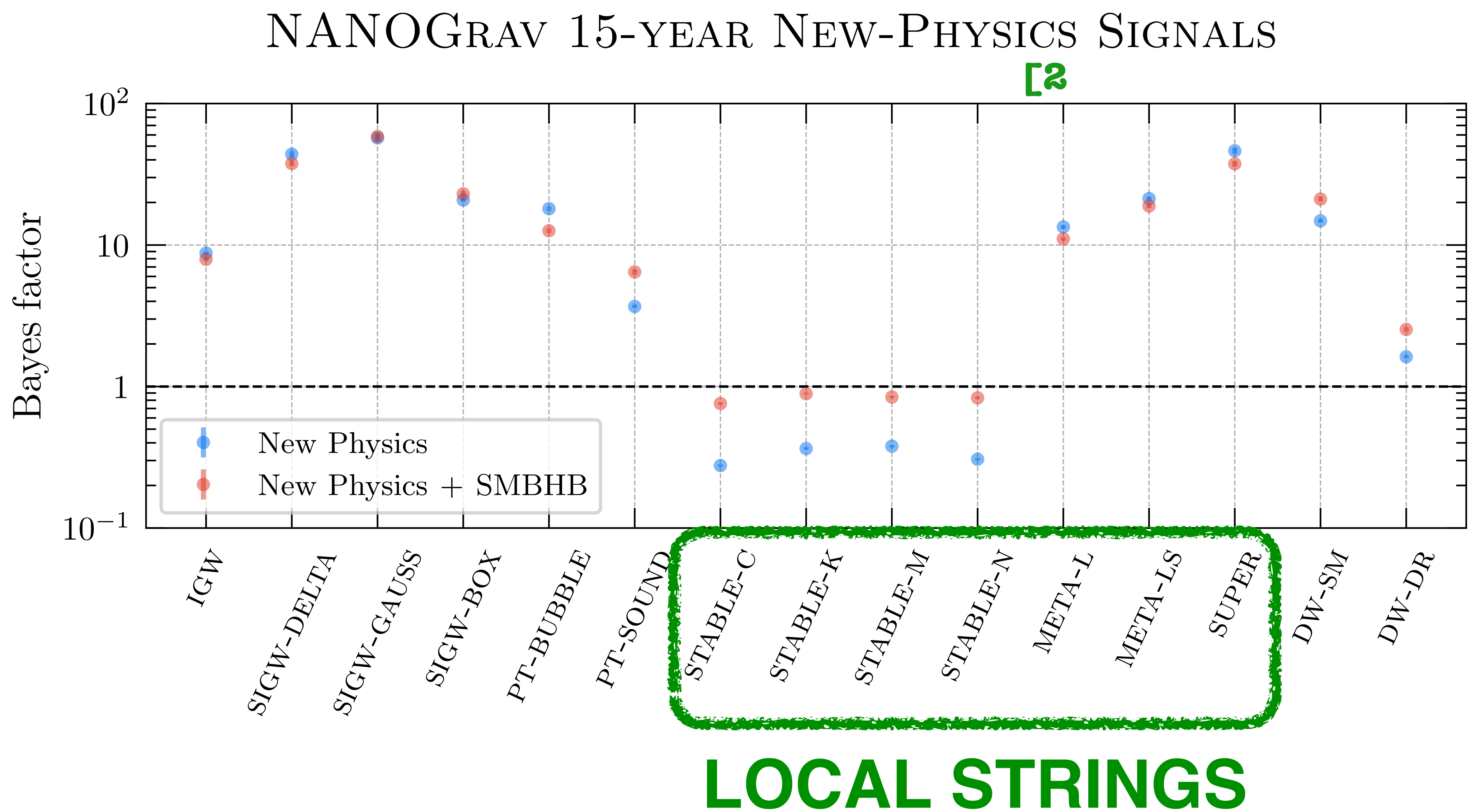

No analysis of global strings in the other PTA papers either.

LOCAL STRINGS vs GLOBAL STRINGS.

See comparison in Appendix F of [1912.02569] .

Loops from global strings : short-lived

Loops from local strings : long-lived.

—> different GW spectra in both frequency and amplitude.

LOCAL STRINGS vs GLOBAL STRINGS.

Global strings: no gauge field, instead massless Goldstone mode, with logarithmically-divergent gradient energy.

Loops quickly decay into axion particles.

GW are mainly produced at the time of the loop production.

$$\Omega_{\rm GW}^{\rm local} \simeq \Omega_r \frac{\eta}{M_{\rm pl}}, \qquad \Omega_{\rm GW}^{\rm global} \simeq \Omega_r \left(\frac{\eta}{M_{\rm pl}}\right)^4 \log^3\left(\eta t_i\right).$$

$\eta = f_a$

LOCAL STRINGS versus GLOBAL STRINGS (m_a=0)

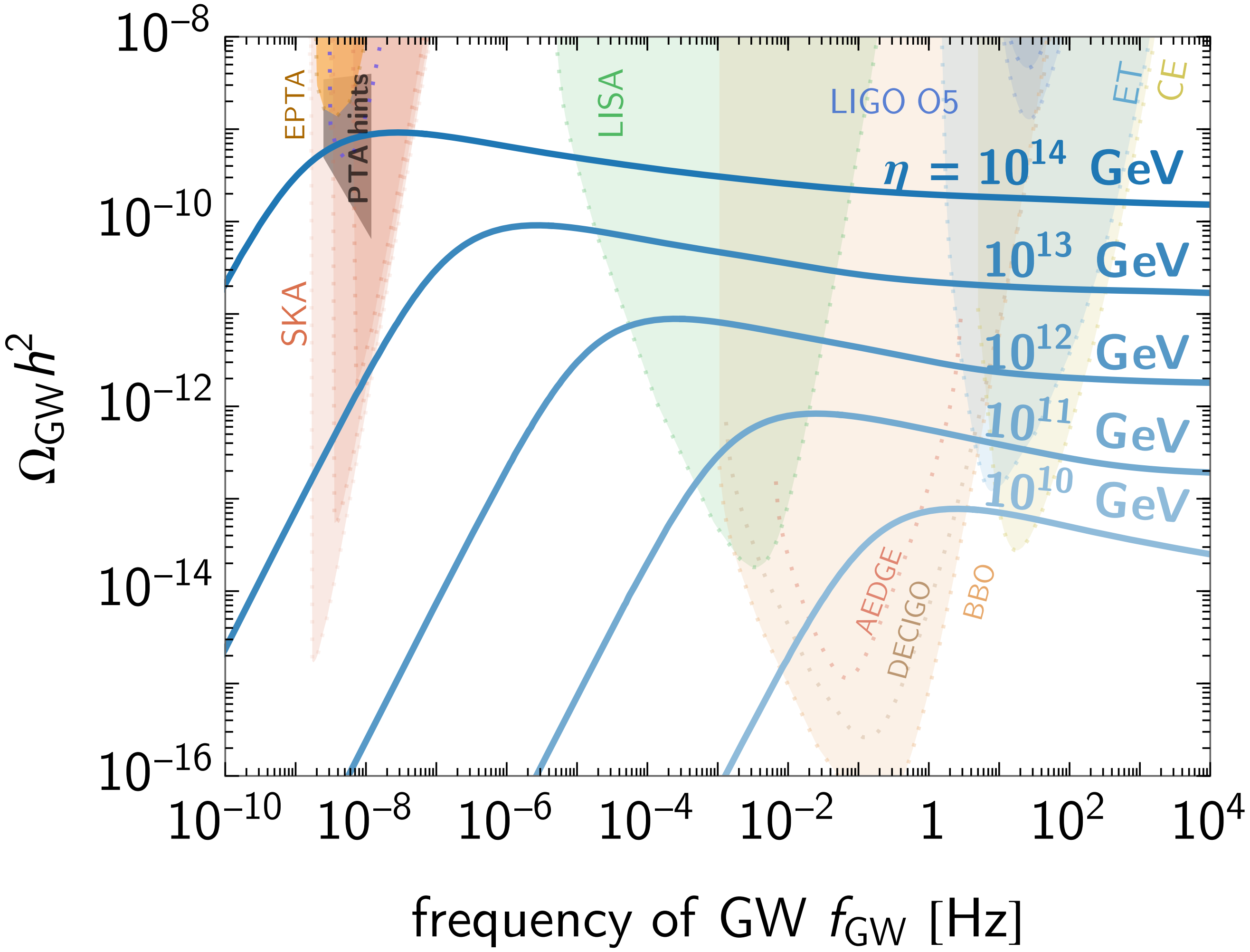

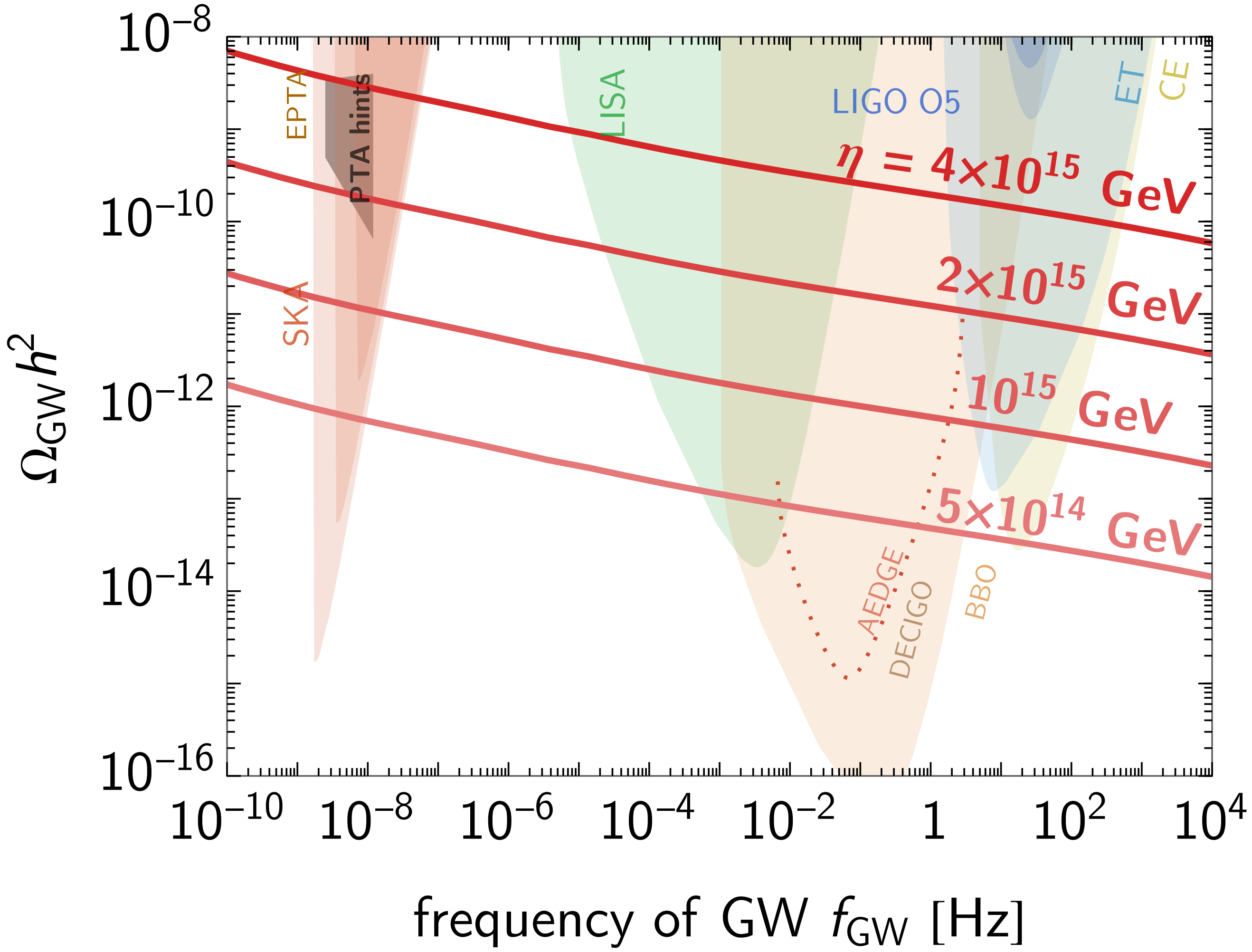

spectral shape changes with η

local loops live longer before decaying (& lifetime depends on η)

global loops decay fast.

To reach the same amplitude as the local strings, global strings need a larger η since GW production is not the leading energy loss.

Temperature-frequency relation.

A loop population produced at temperature T quickly decays into GW of frequency

$$f_{\rm GW}^{\rm cs}(T) \simeq 63\ {\rm nHz} \left(\frac{\alpha}{0.1}\right) \left(\frac{T}{10{\rm MeV}}\right) \left[\frac{g_*(T)}{10.75}\right]^{\frac{1}{4}},$$

α: typical loop size in units of Hubble horizon

IR cutoff of GW spectrum fixed by axion mass

Network decays when H ~ m_a

$$f_{\rm GW}^{\rm cs}(m_a) \simeq 9.4\ {\rm nHz}\left(\frac{\alpha}{0.1}\right)\left(\frac{m_a}{10^{-15}{\rm eV}}\right)^{\frac{1}{2}}.$$

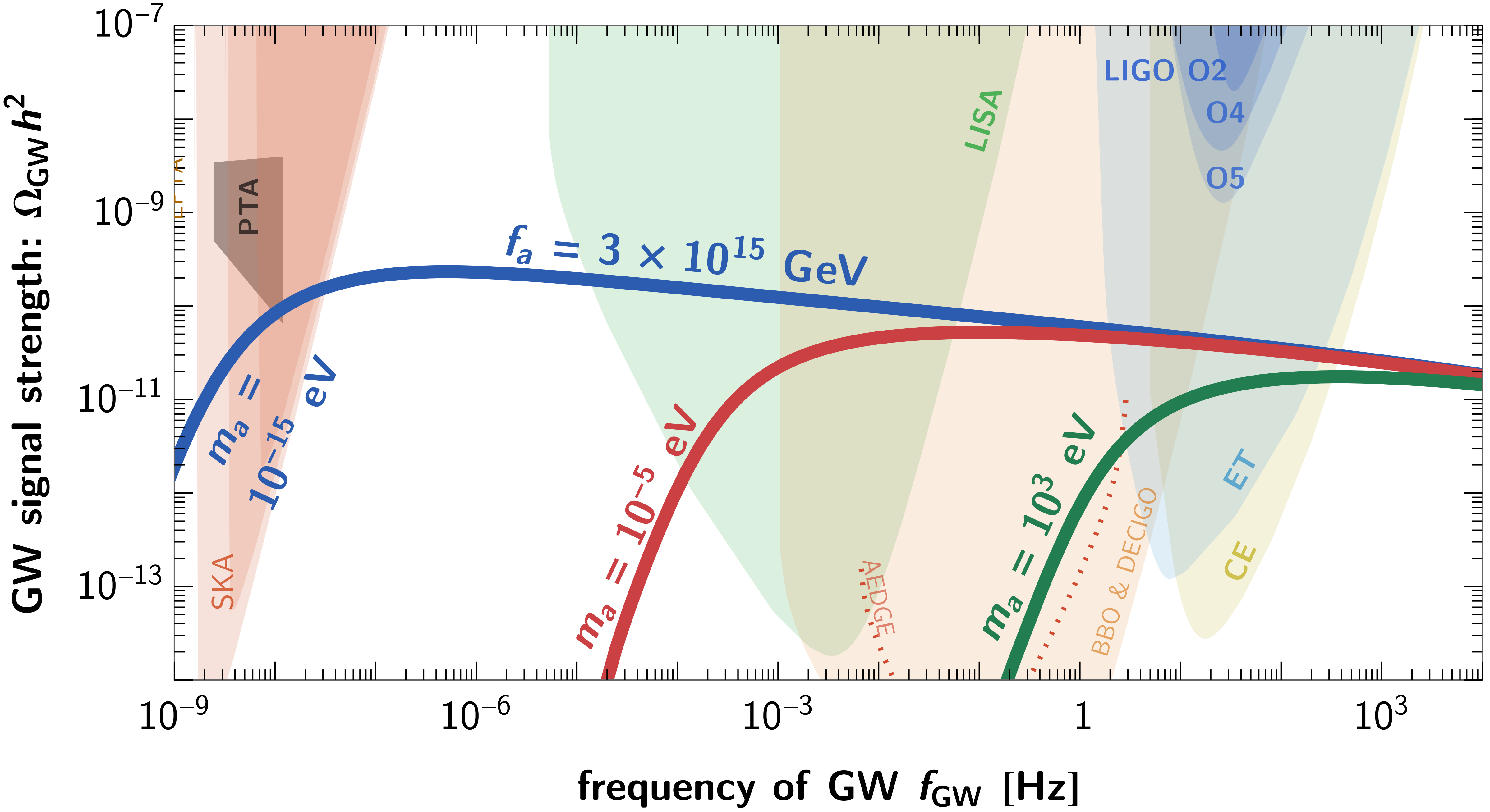

Analysis of 15 year-NANOGrav data .

[Servant, Simakachorn, 2307.03121

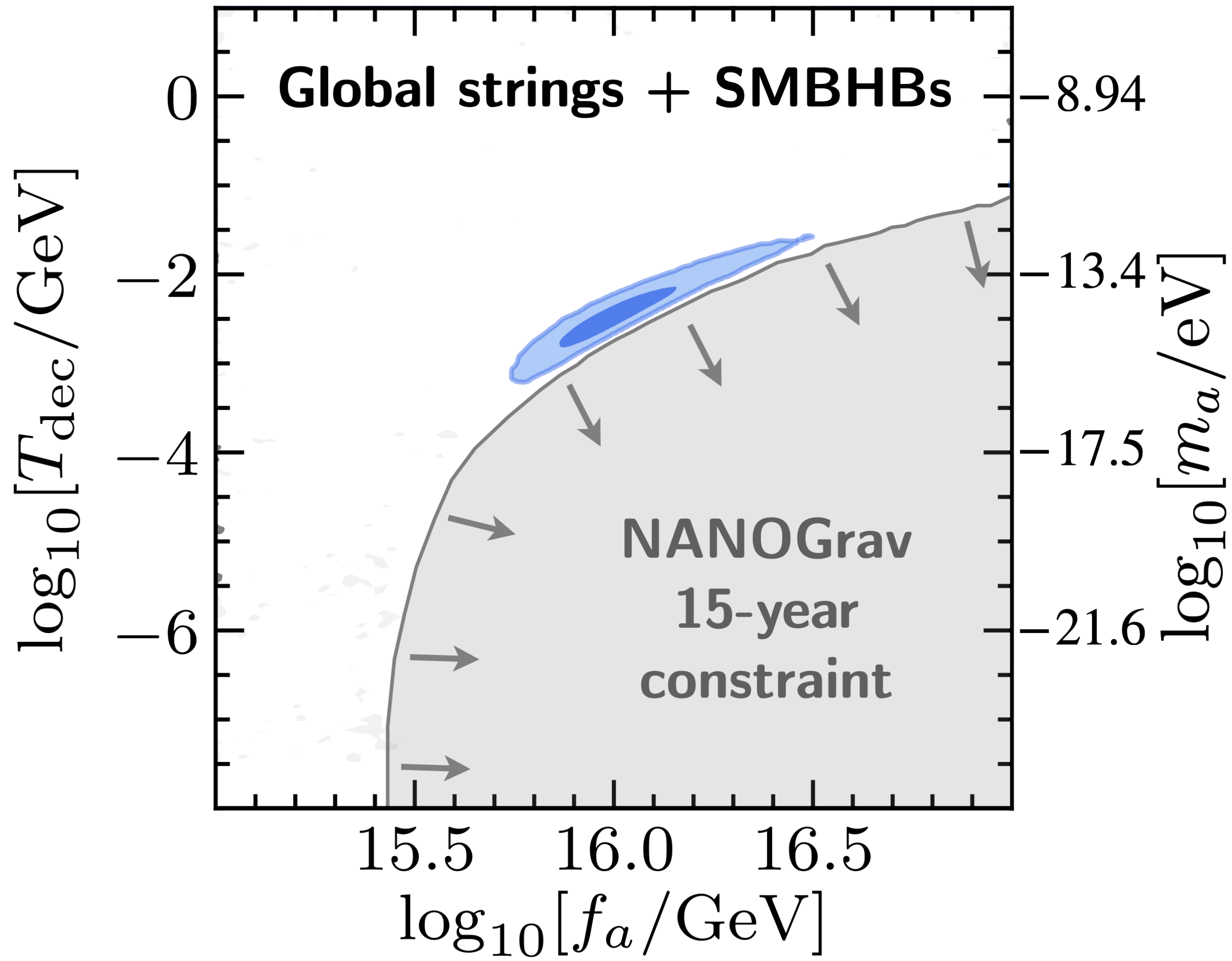

Best-fitted spectra to PTA data:

{fa, ma} ≃ {9.9 · 10^{15} GeV, 4.8 · 10^{-15} eV})

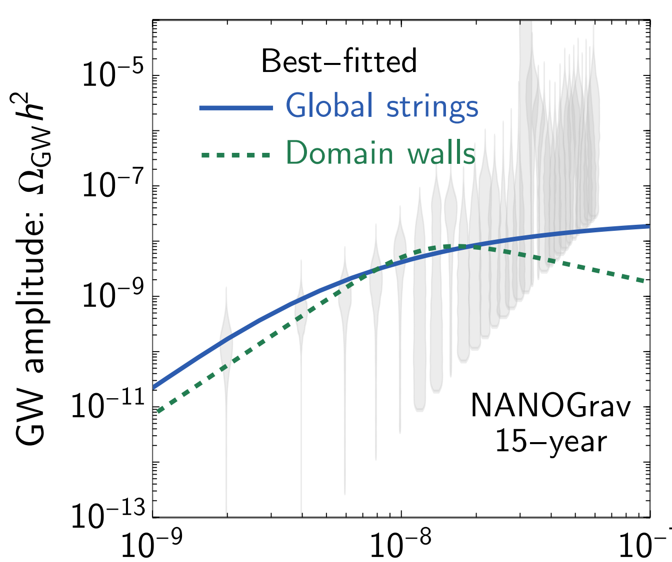

Without the SMBHBs

Best-fit does not change much $\{f_a, m_a\} = \{9.55 \cdot 10^{15}\ \text{GeV}, 3.89 \cdot 10^{-15}\ \text{eV}\}$

$$\text{BF} \simeq 22.8$$

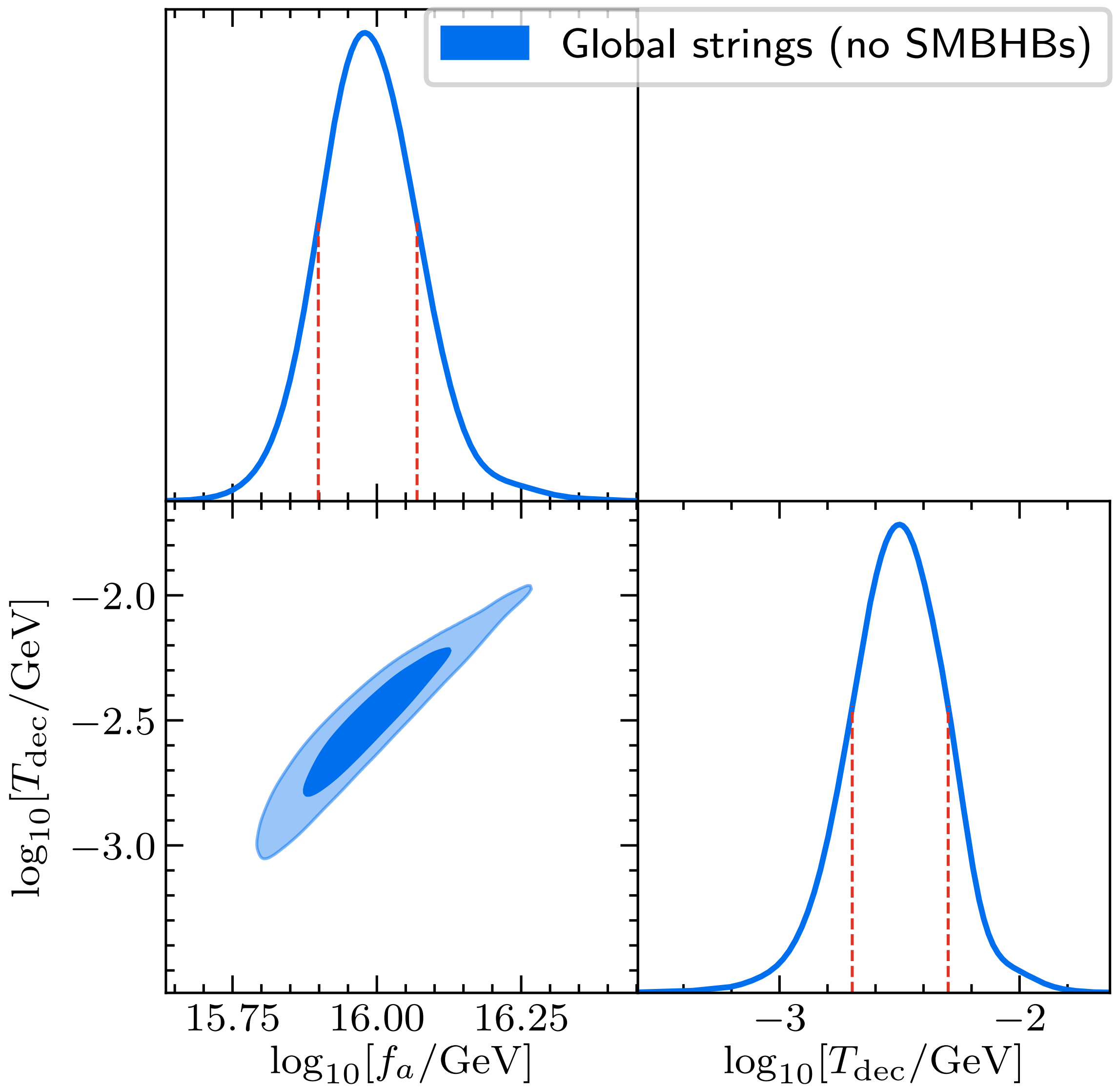

Massless limit .

$$m_a \ll 10^{-16}\ \mathrm{eV}$$

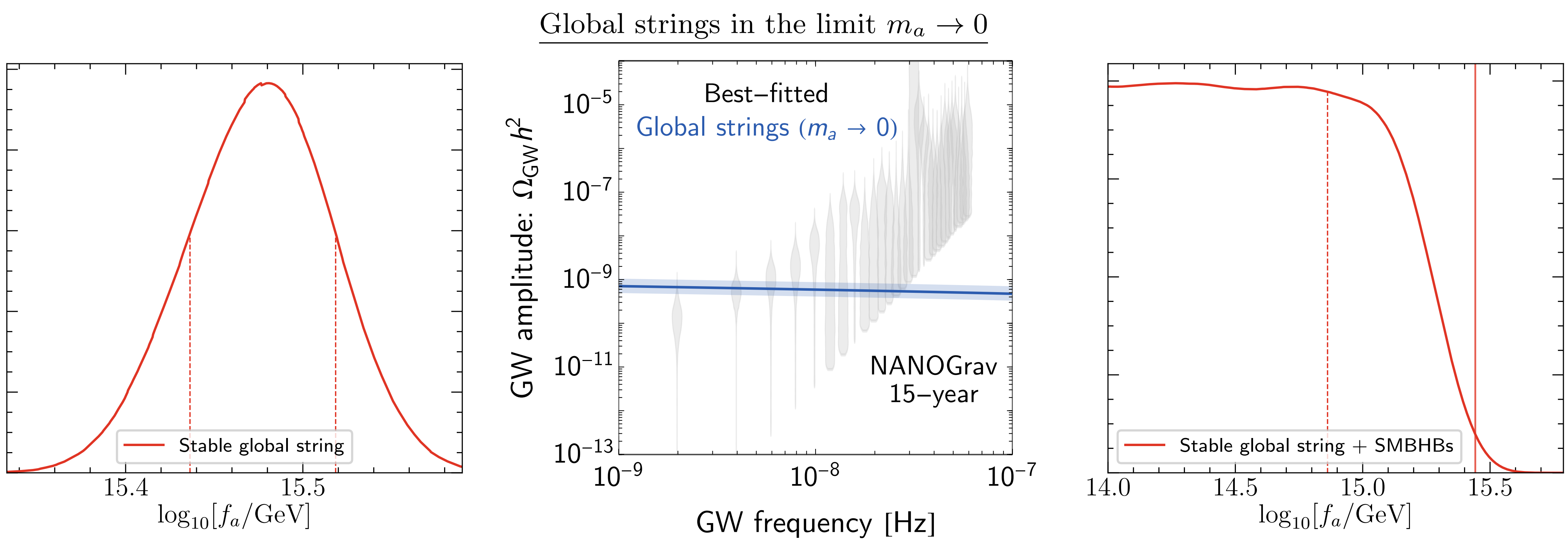

BF=1.45×10^{-3} (without SMBHBs)

BF= 0.64 (with SMBHBs)

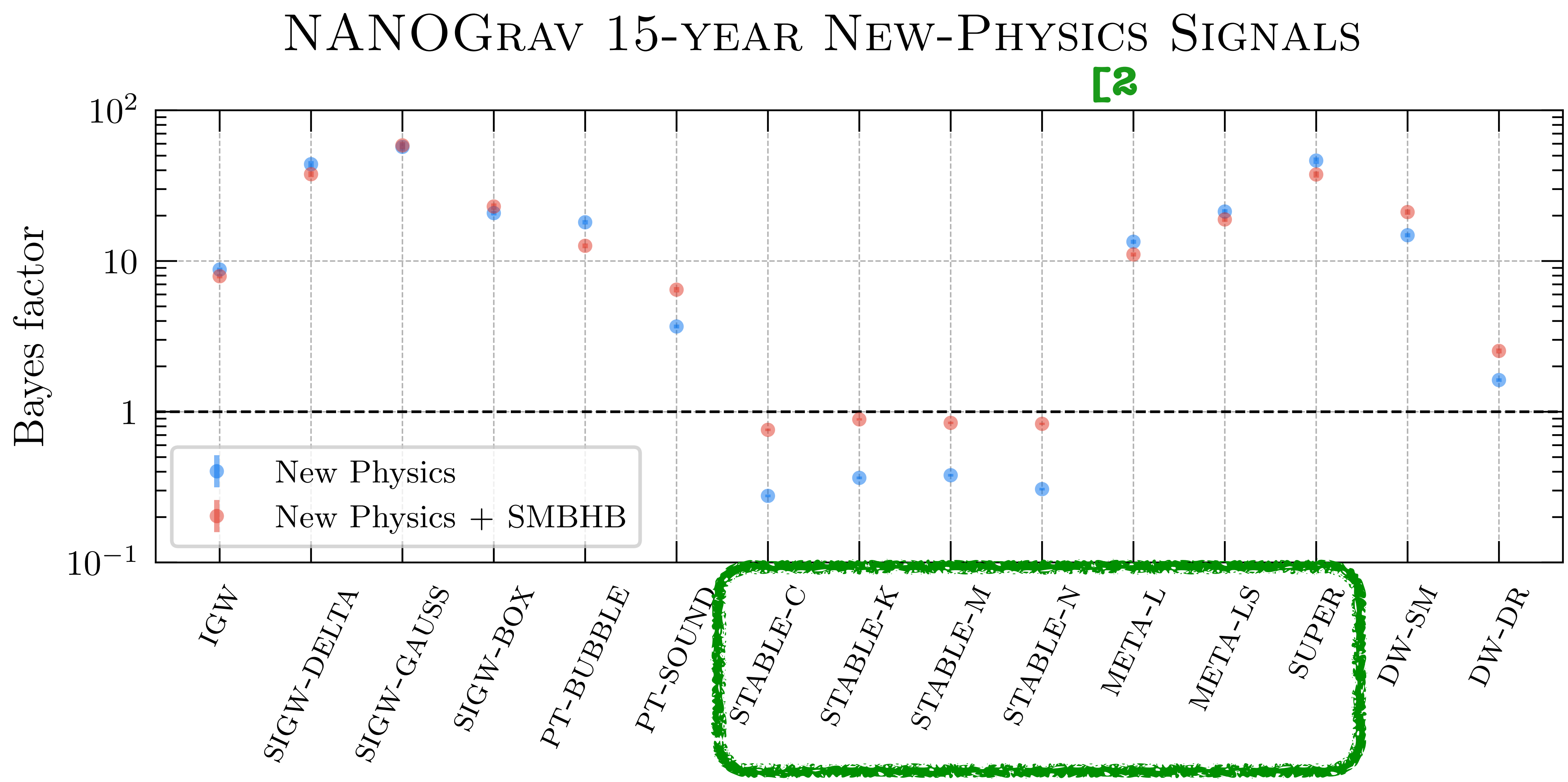

LOCAL STRINGS

No analysis of global strings in the other PTA papers either.

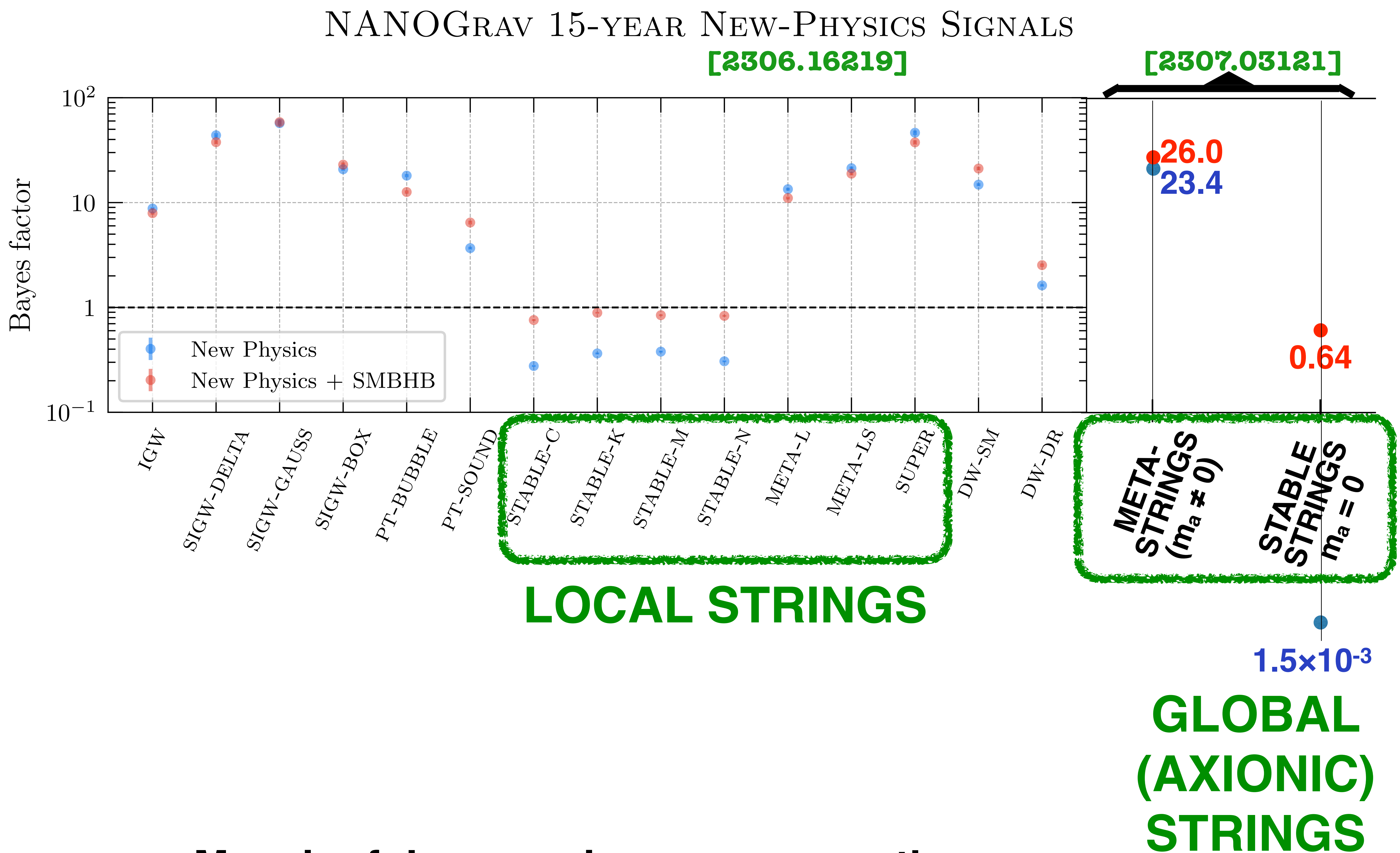

Meaningful comparison as we use the same SMBHB model as in the NG15 paper.

Translating the new constraint in the (m_a, f_a) plane

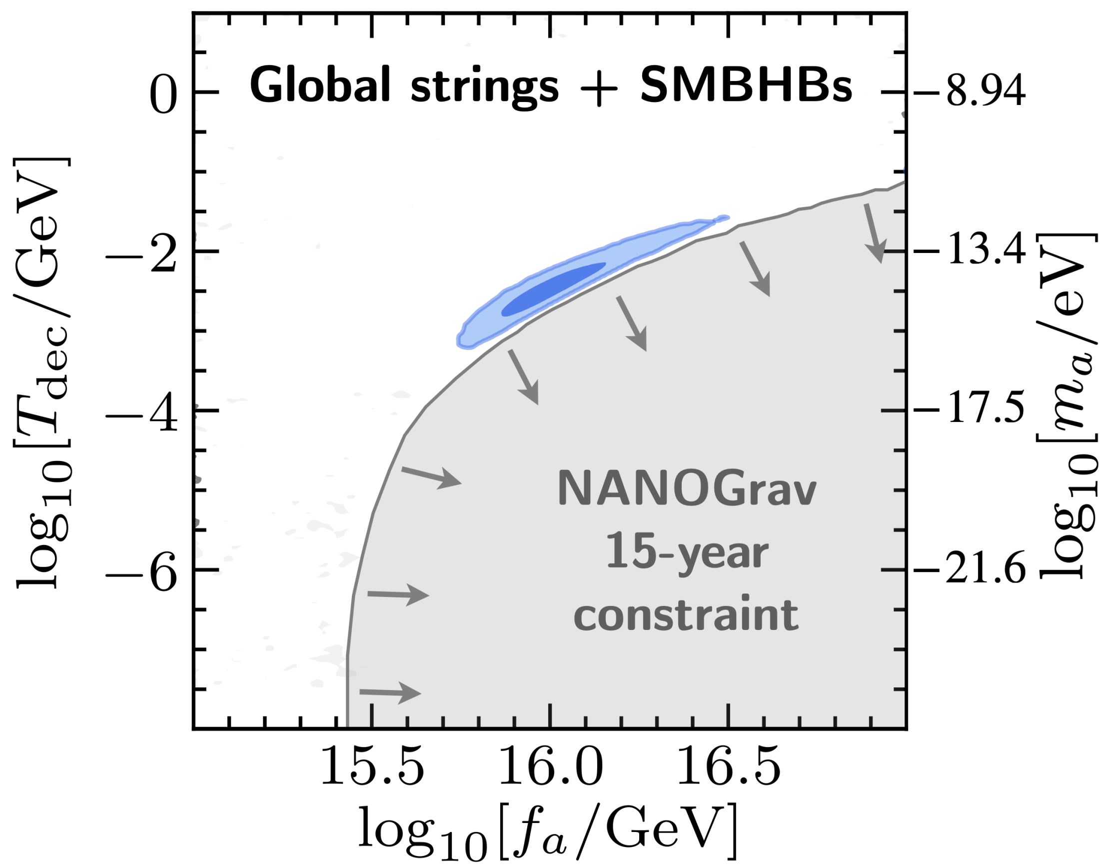

Lab bounds

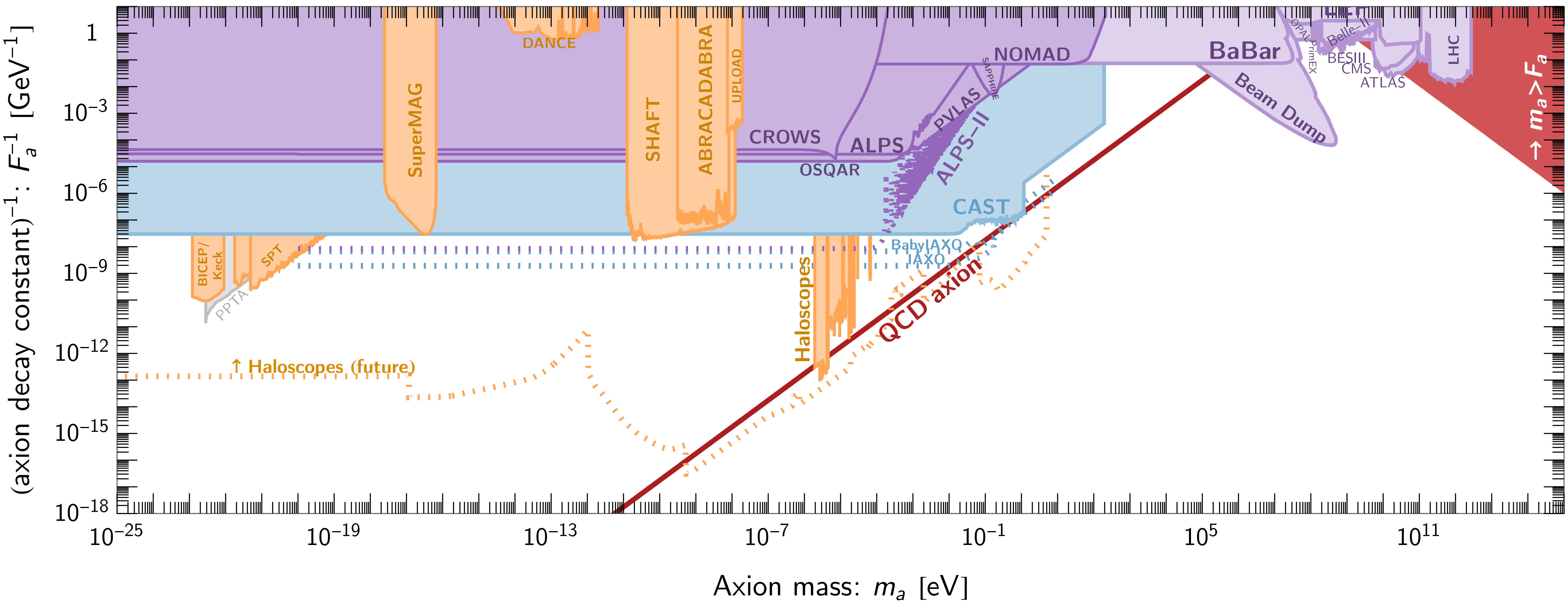

DANCE
SuperMAG
SHAFT
ABRACADABRA
UPLOAD
CROWS
OSQAR
ALPS
NOMAD
SAPPHIRE
PVLAS
ALPS–II
CAST
BabyIAXO
IAXO
BaBar
Beam Dump
Belle–II
BESIII
CMS
ATLAS
LHC
$\to m_a > F_a$
BICEP/ Keck
SPT
PPTA
Haloscopes
↑ Haloscopes (future)
QCD axion
(axion decay constant)$^{-1}$: F_a^{-1} [GeV^{-1}]
Axion mass: m_a [eV]

Adding astro bounds .

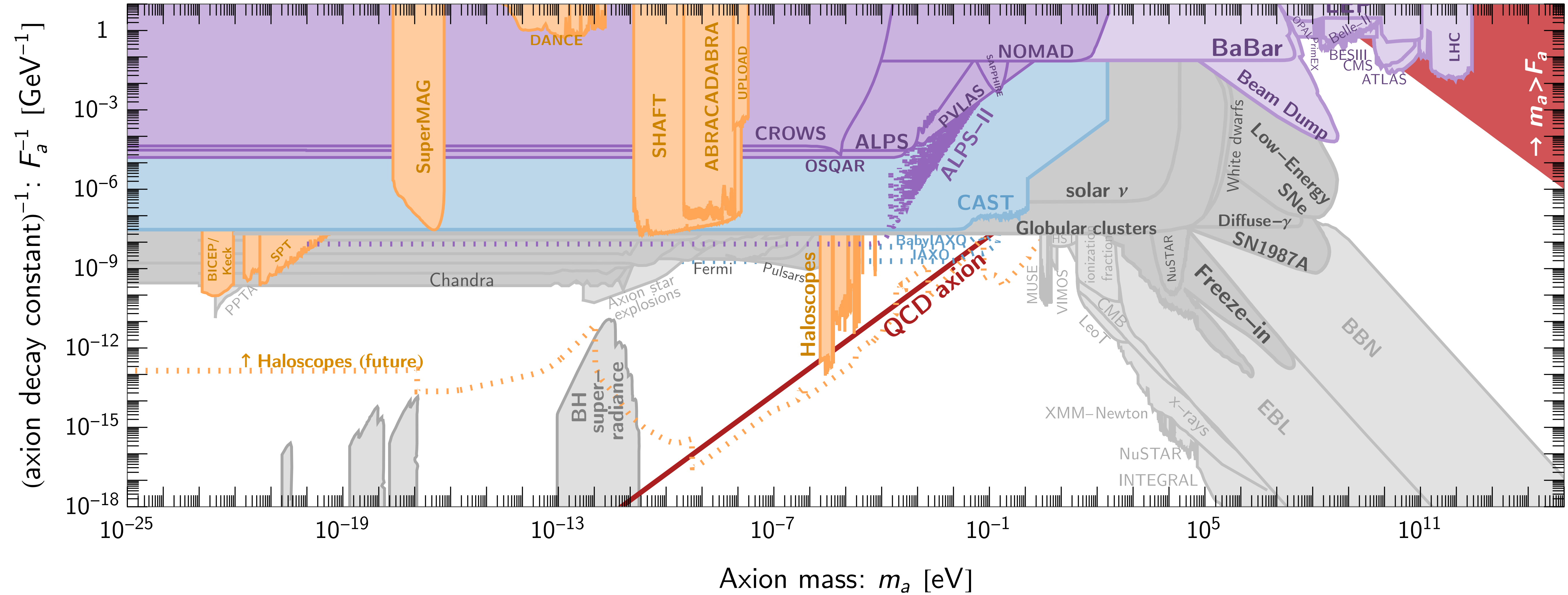

Theoretical bound from ALP abundance

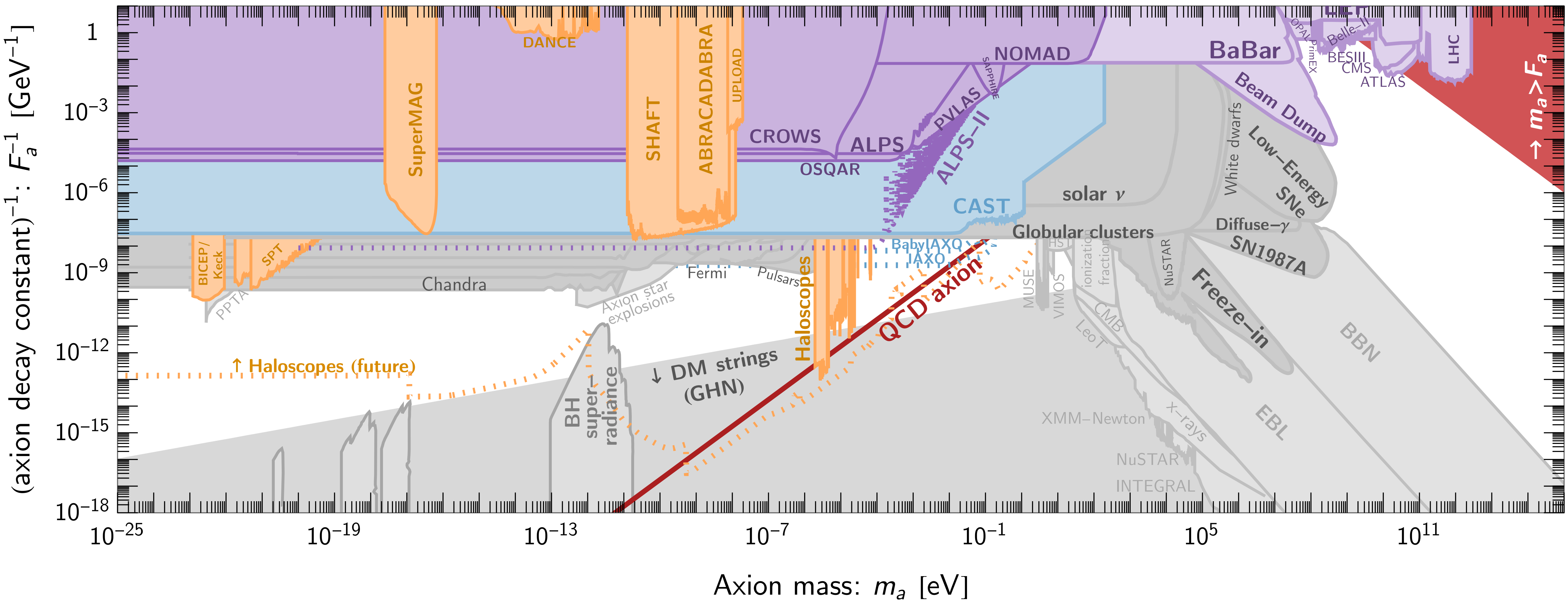

N_{eff} bound from ALP abundance

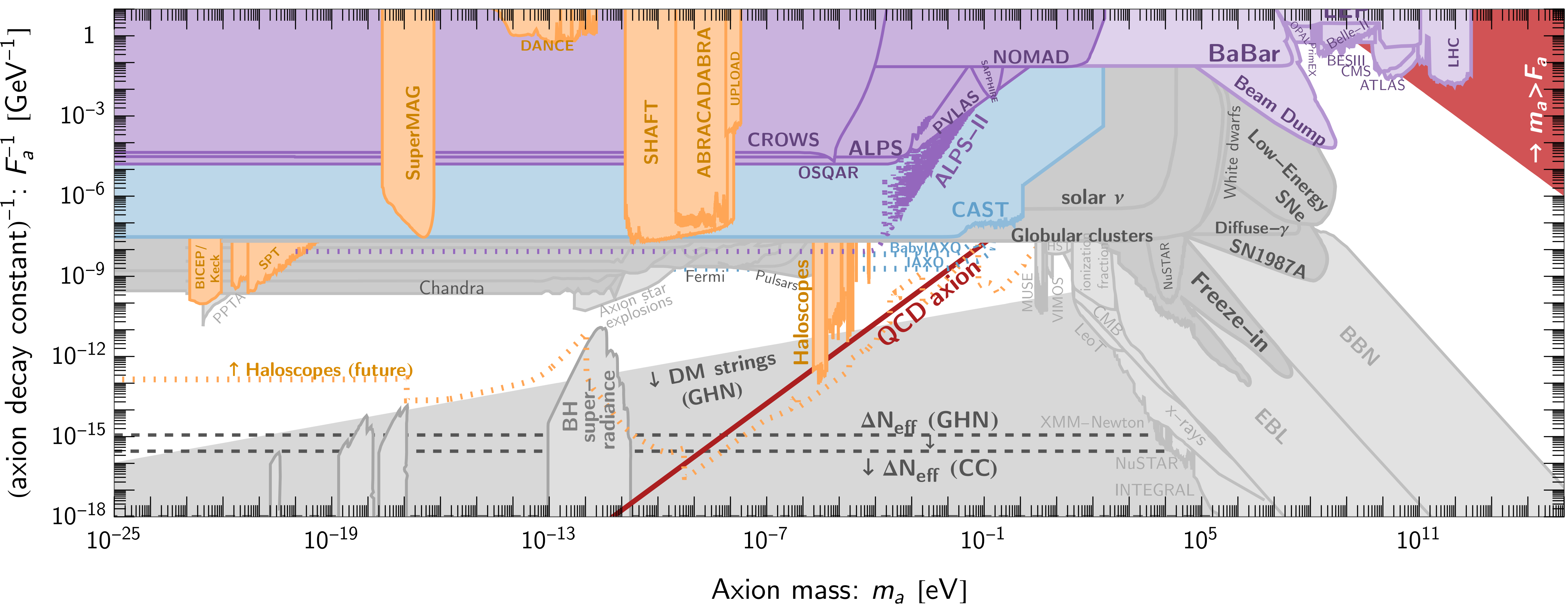

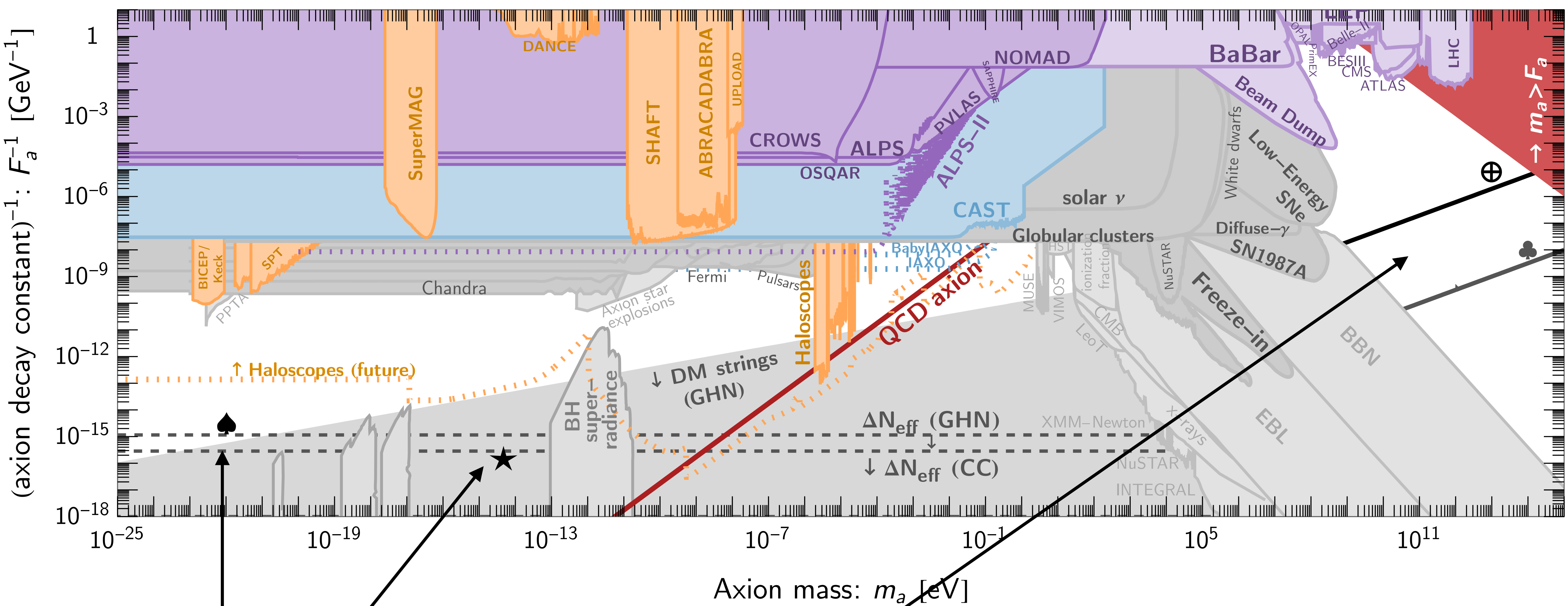

Benchmark spectra

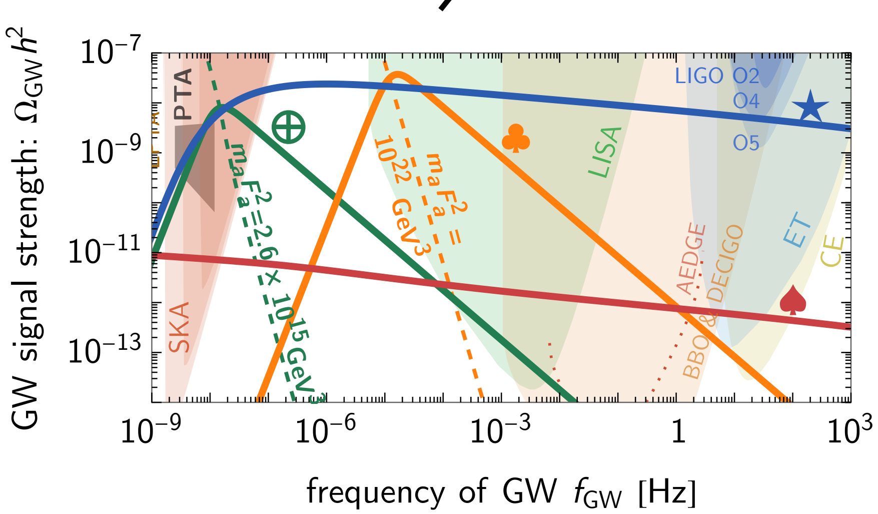

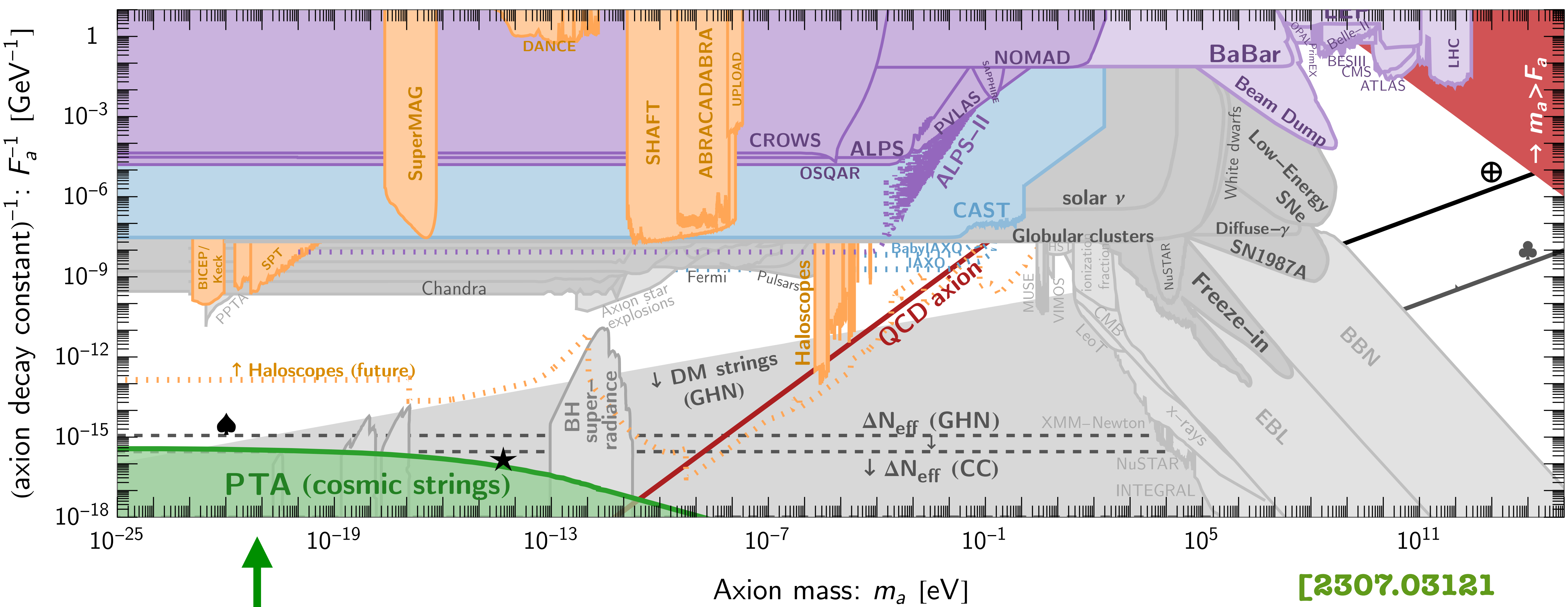

[2307.03121

New PTA constraint

Domain Wall contribution

Scalar potential.

$\Phi \equiv \phi \exp(i\theta)$ with ϕ the radial partner

$$V(\Phi) = \underbrace{\frac{\lambda}{2}(\phi^2 - f_a^2)^2}_{\text{cosmic strings}} + \underbrace{\frac{m_a^2 f_a^2}{N_{\rm DW}^2}\left[1 - \cos\left(N_{\rm DW}\theta\right)\right]}_{\text{domain walls}} + V_{\rm bias},$$

For $N_{DW} > 1$: Domain wall contribution to the GW bgd.

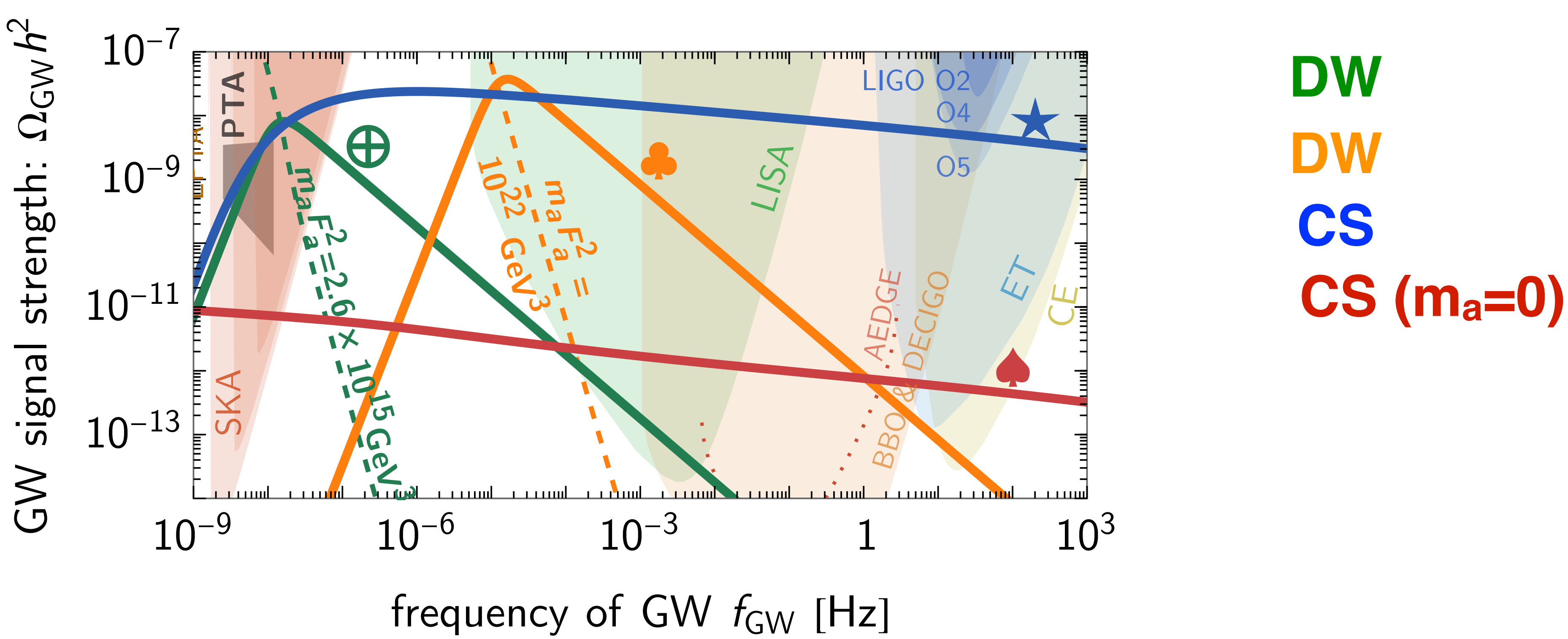

String-wall system collapses at temperature

$$T_\star \simeq 53\text{MeV} \left[\frac{10.75}{g_*(T_*)}\right]^{\frac{1}{4}} \left[\frac{V_{\text{bias}}^{\frac{1}{4}}}{10\text{MeV}}\right]^2 \left[\frac{\text{GeV}}{m_a}\right]^{\frac{1}{2}} \left[\frac{10^6\text{GeV}}{f_a/N_{\text{DM}}}\right].$$

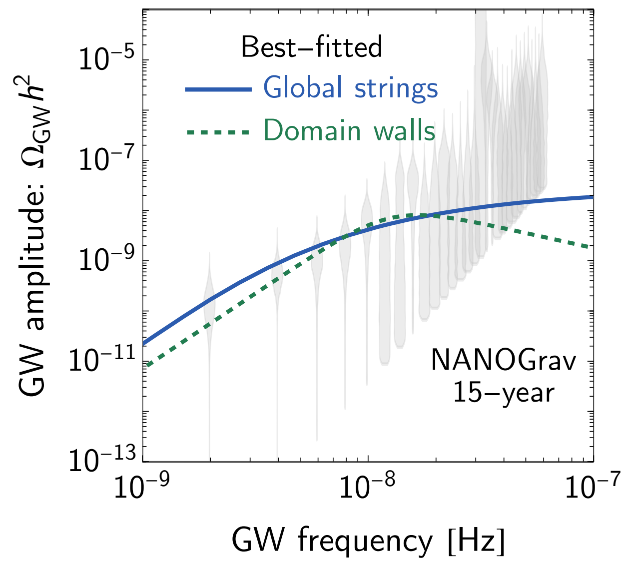

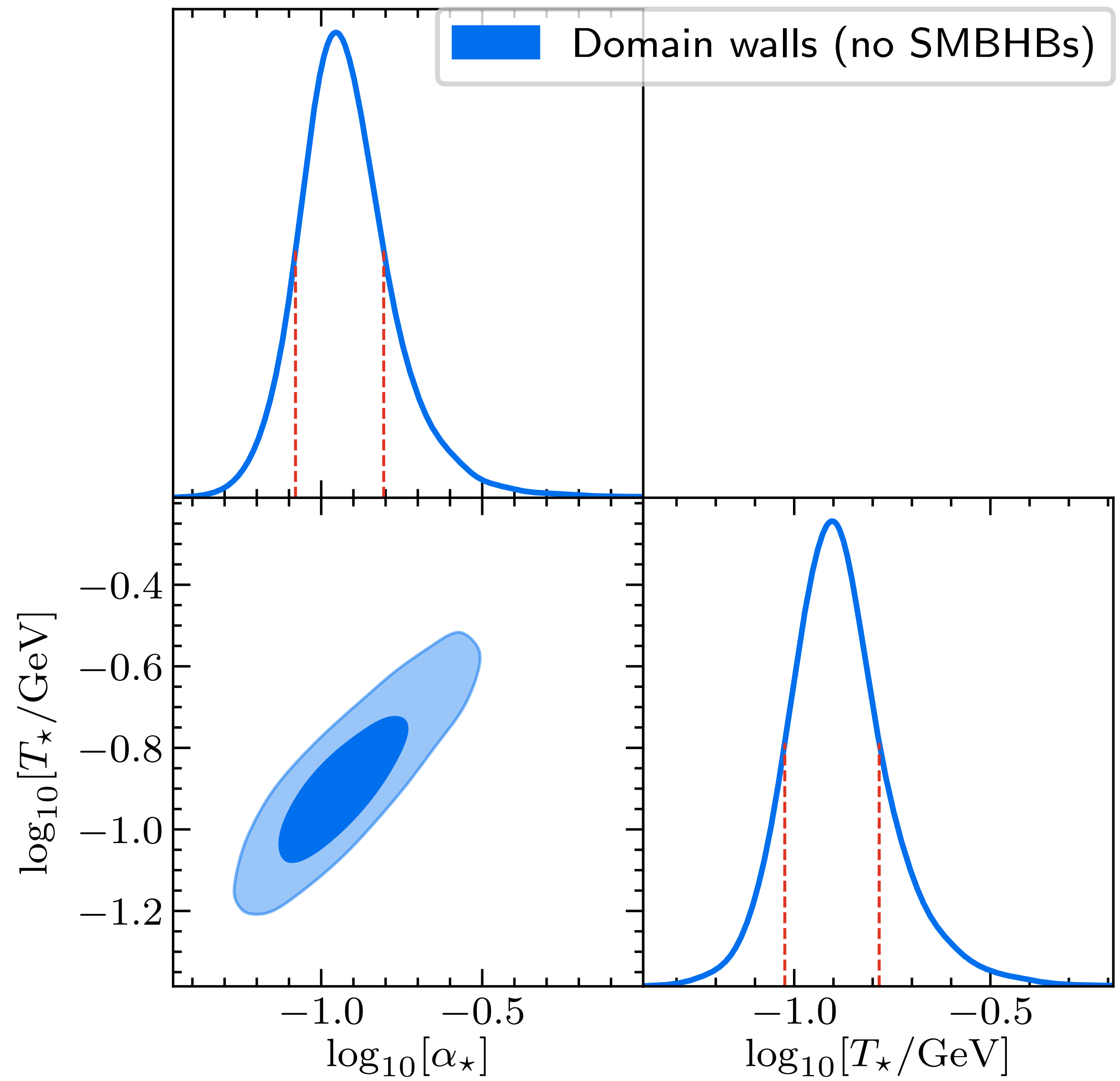

BF ~ 23.4 without SMBHB

BF ~ 44.7 with SMBHB

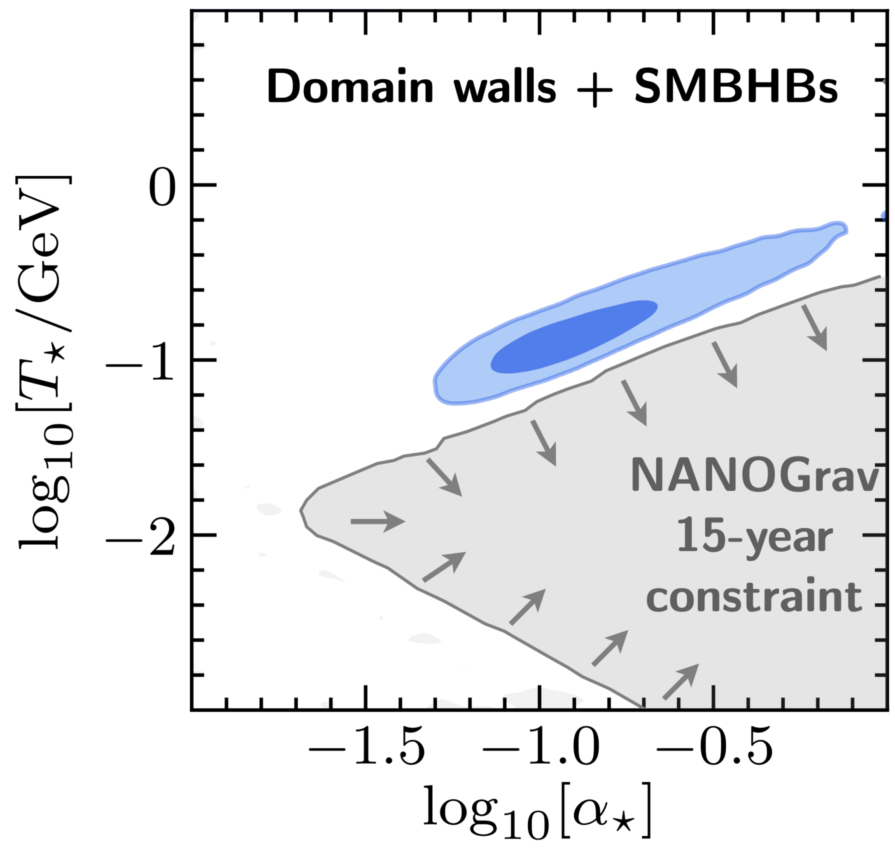

Domain walls + SMBHBs
NANOGrav
15-year
constraint
$\log_{10}[T_\star/\mathrm{GeV}]$
$\log_{10}[\alpha_\star]$

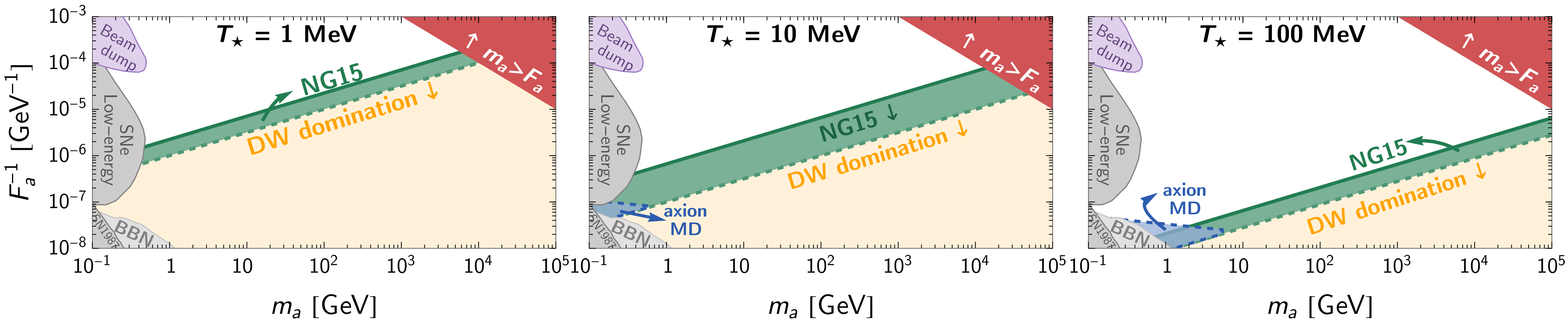

$T_\star$ = 1 MeV
$T_\star$ = 10 MeV
$T_\star$ = 100 MeV
Beam dump
SNe
Low-energy
BBN
NG15
DW domination ↓
axion MD
↑ $m_a > F_a$
F_a^{-1} [GeV^{-1}]
m_a [GeV]

[2307.03121]

Constraining post-inflationary axions with Pulsar Timing Arrays .

[2307.03121

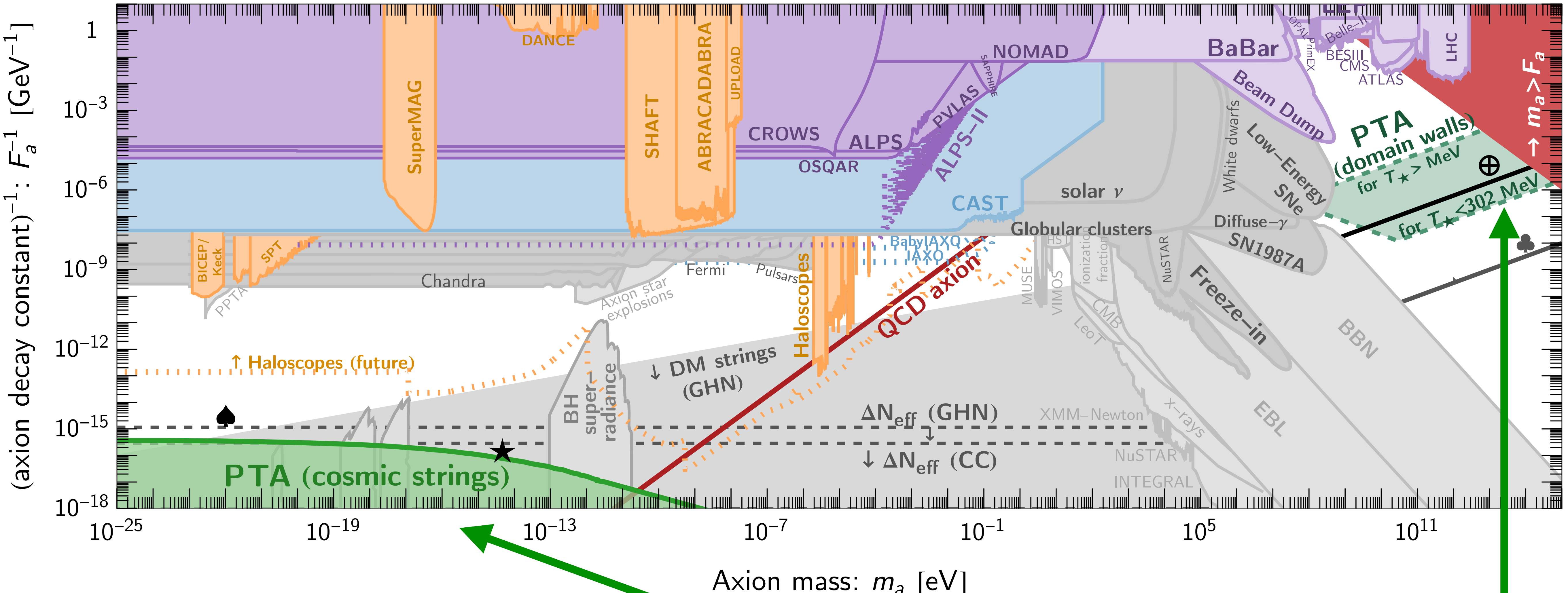

New PTA constraints

GWs
from axion fragmentation.

The transfer of energy in the early universe from the homogeneous axion field into axion quantum fluctuations, e.g. axion fragmentation, inevitably produces a stochastic background of gravitational waves of primordial origin with a peak frequency controlled by the axion mass.

$$\ddot{h}_{ij} + 3H\dot{h}_{ij} - \frac{\Delta h_{ij}}{a^2} = \frac{16\pi}{M_{\rm pl}^2}\Pi_{ij}^{\rm TT},$$

$$\Pi_{ij}^{\rm TT}(t,\vec{x}) = \frac{1}{a^2}\left[\partial_i\phi(t,\vec{x})\partial_j\phi(t,\vec{x}) - \frac{1}{3}\delta_{ij}(\partial_k\phi(t,\vec{x})\partial_k\phi(t,\vec{x}))\right]$$

Examples.

Machado et al, 1811.01950

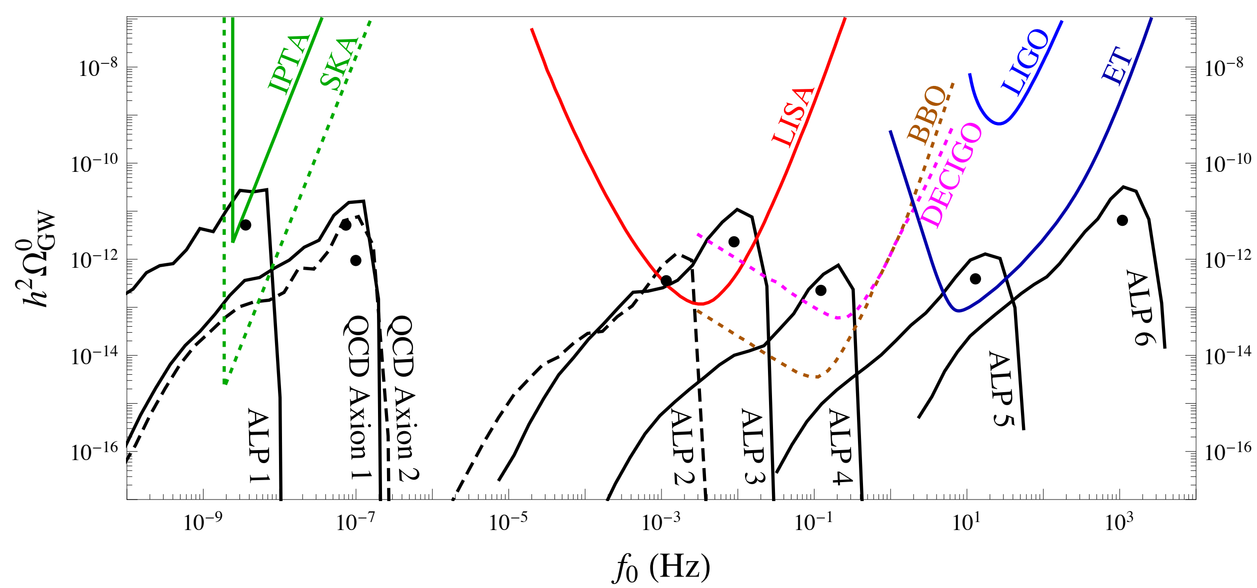

Chatrchyan, Jaeckel 2004.07844

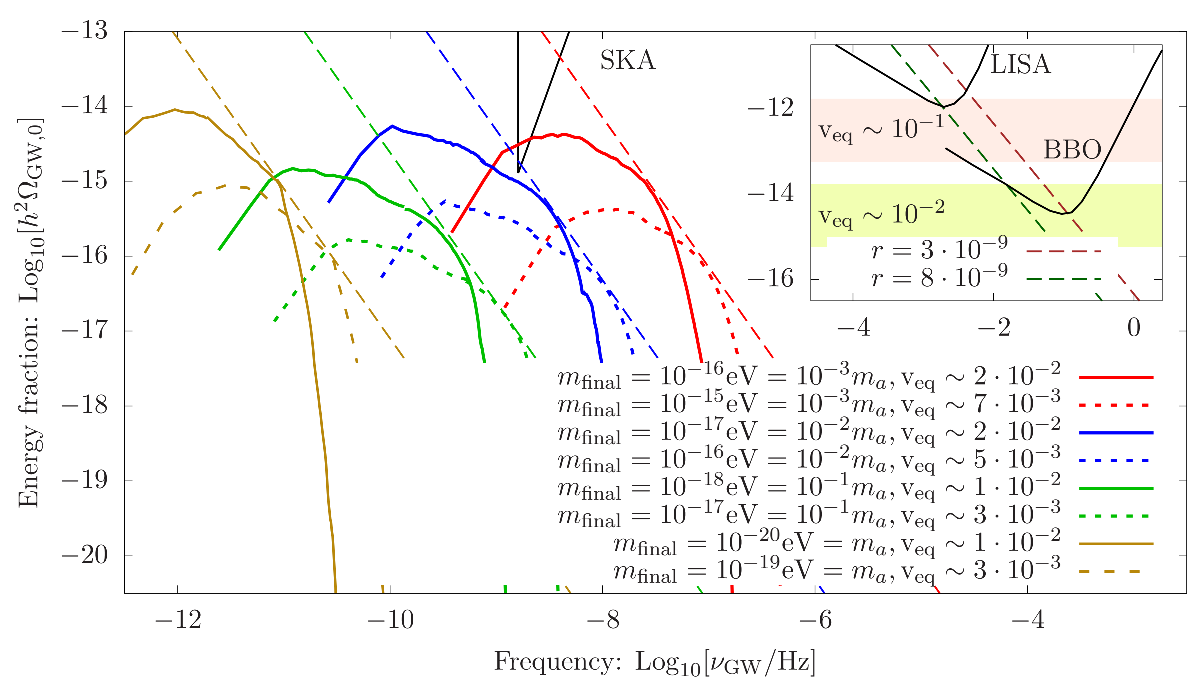

The signal is generally suppressed when imposing the upper bounds from either the axion dark matter abundance or the axion dark radiation.

Schwaller et al, 2012.11584 (from coupling to dark photon)
Eroncel et al, 2206.14259
Geller et al, 2307.03724

—>Dilution of ALP energy density needed

Achieved dilution factor of ALP energy density

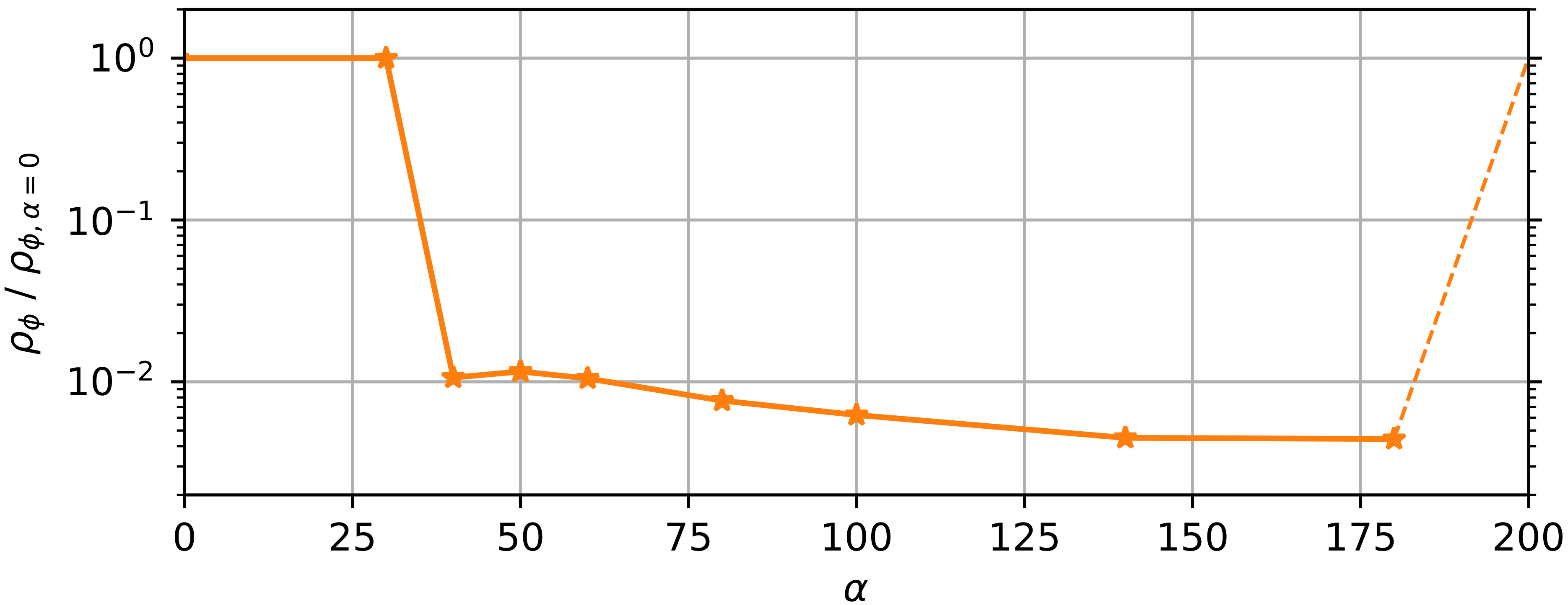

Ratzinger, Schwaller, Stefanek, 2012.11584

$\mathcal{Z}$ = needed dilution factor of ALP energy density

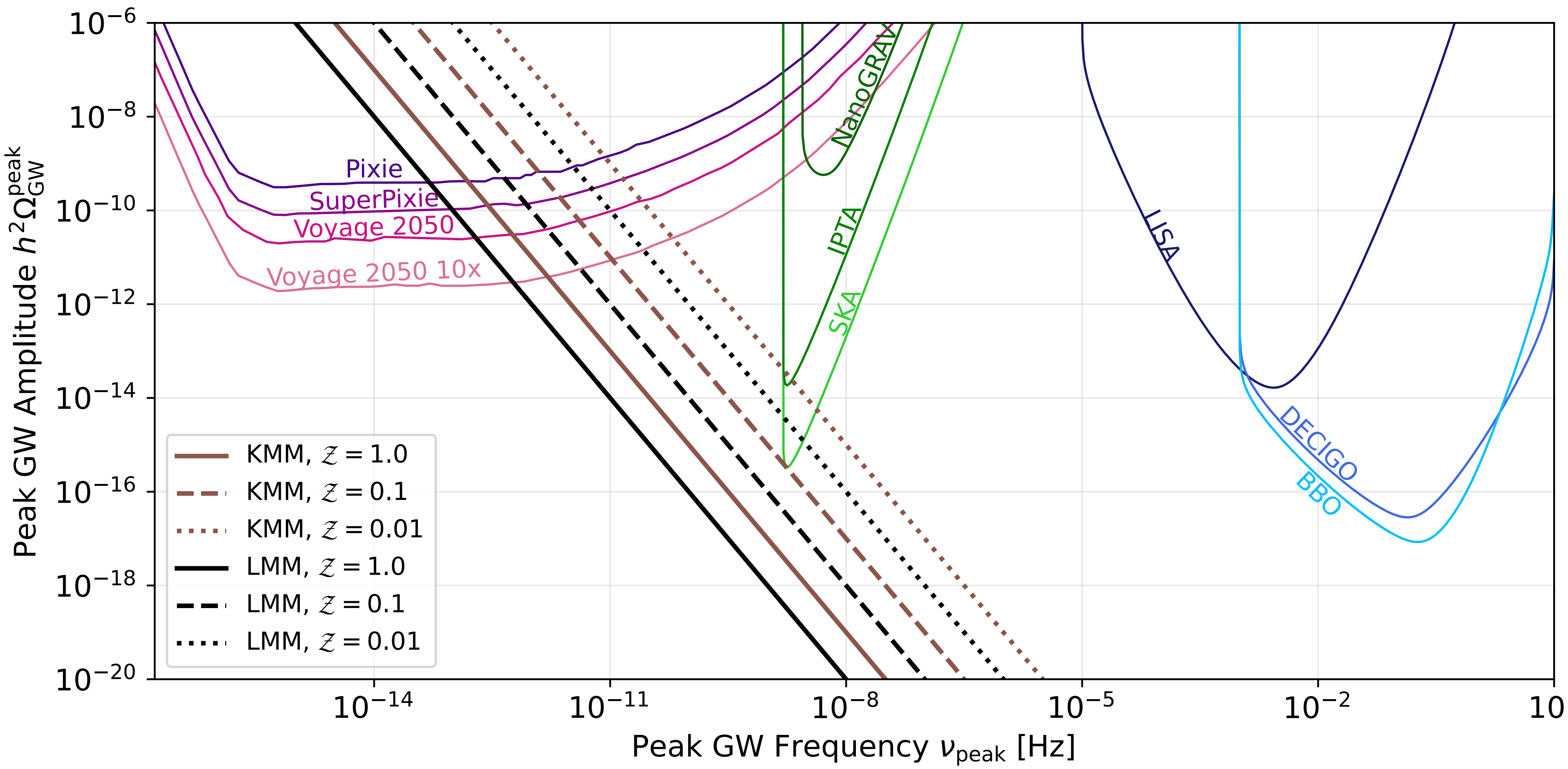

Eroncel et al, 2206.14259

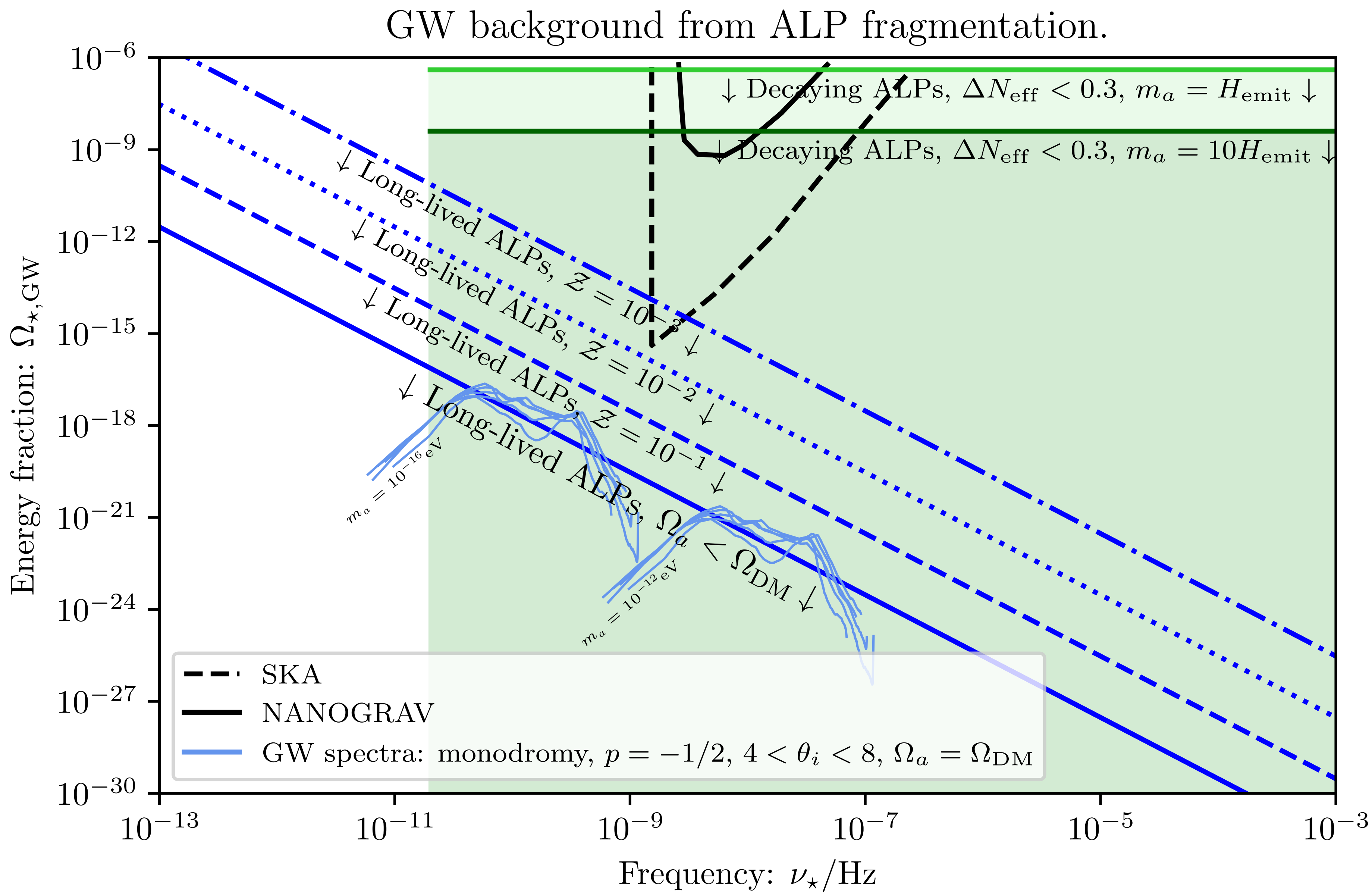

Chatrchyan & al, in prep.

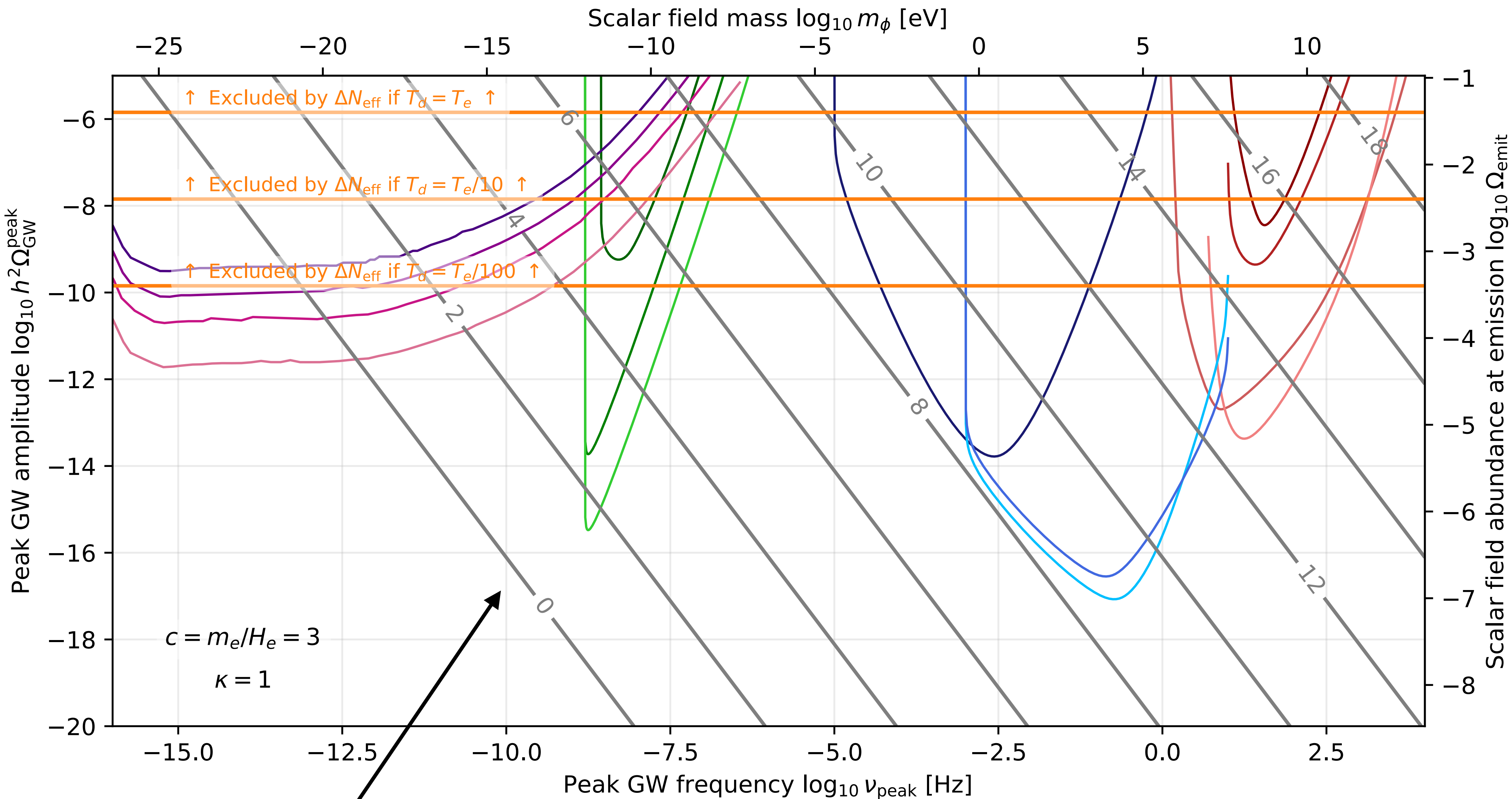

10ᵃ : required dilution factor

Chatrchyan & al, in prep.

Extra material.

SOME REFERENCES

GW from GLOBAL CS:

Chang & Cui, [1910.04781], [2106.09746].

Gouttenoire et al,[1912.02569].

Gorghetto, Hardy & Nicolaescu, [2101.11007].

Ramberg & Visinelli, [1904.05707], [2012.06882].

GW from DW:

T. Hiramatsu, M. Kawasaki and K. Saikawa, On the estimation of gravitational wave spectrum from cosmic domain walls, JCAP 02 (2014) 031 [1309.5001].

R. Zambujal Ferreira, A. Notari, O. Pujolas & F. Rompineve, High Quality QCD Axion at Gravitational Wave Observatories, Phys. Rev. Lett. 128 (2022) 141101 [2107.07542].

K. Saikawa, Gravitational waves from cosmic domain walls: a mini-review, J. Phys. Conf. Ser. 1586 (2020) 012039.

. R. Z. Ferreira, A. Notari, O. Pujolas and F. Rompineve, Gravitational waves from domain walls in Pulsar Timing Array datasets, JCAP 02 (2023) 001 [2204.04228].

. E. Madge, E. Morgante, C. P. Iba´n˜ez, N. Ramberg and S. Schenk, Primordial gravitational waves in the nano-Hertz regime and PTA data – towards solving the GW inverse problem, 2306.14856.

GW from cosmic strings.

GW spectrum

⇨ GW emission from a loop × loop-number density

$$\Omega_{\rm GW}^{(k)}(f) = \frac{1}{\rho_c} \cdot \frac{2k}{f} \cdot \frac{(0.1)\Gamma^{(k)} G\mu^2}{\alpha(\alpha + \Gamma G\mu)} \int_{t_F}^{t_0} d\tilde{t} \frac{C_{\rm eff}(t_i)}{t_i^4} \left[\frac{a(\tilde{t})}{a(t_0)}\right]^5 \left[\frac{a(t_i)}{a(\tilde{t})}\right]^3 \Theta(t_i - t_F)$$

string's nature — loop number — red-shift

a^{-3}

GW: a^{-4}, loop size: a^{-1}

$t_i \equiv$ loop production, $\tilde{t} \equiv$ loop emission cosmic string (local)

loop production @ t_i loop emission @ t_*

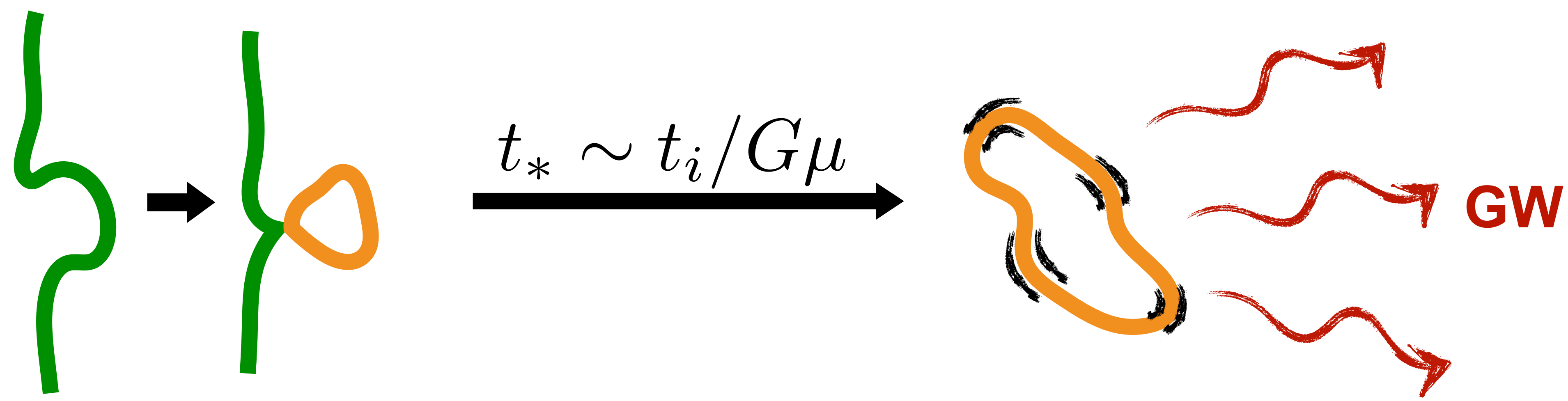

Relation between observed frequency & Hubble radius at emission

$$f \approx H_* \left(\frac{a_i}{a_0}\right) \left(\frac{1}{G\mu}\right)^{1/2}$$

With respect to local strings, the GW spectrum from global strings in standard radiation cosmology is:

- suppressed by the shorter Hubble time $\tilde{t}_M$ at the time of GW emission: factor $\tilde{t}_{\rm M}^{\rm global}/\tilde{t}_{\rm M}^{\rm local} \propto G\mu_{\rm local} \propto \left(\eta/M_{\rm pl}\right)^2$,
- suppressed by the larger GW redshift factor since emission occurs earlier: factor $\left[\frac{a\left(\tilde{t}_{\rm M}^{\rm global}\right)}{a\left(\tilde{t}_{\rm M}^{\rm local}\right)}\right]^4 \propto \left(\eta/M_{\rm pl}\right)^4$,
- enhanced by the lower loop redshift factor since GW emission occurs right after loop production: factor $\left(a\left(\tilde{t}_{\rm M}^{\rm local}\right)/a\left(\tilde{t}_{\rm M}^{\rm global}\right)\right)^3 \propto \left(\eta/M_{\rm pl}\right)^{-3}$,
- increased by the logarithmically-enhanced GW power emission rate: factor $\log^2\left(\eta t_i\right)$,
- increased by the logarithmically-enhanced loop lifetime: factor $\log\left(\eta t_i\right)$.

Which of these axions can make Dark Matter ?

Axions from the misalignment mechanism.

Start with ALP lagrangian $\mathcal{L} = -\frac{f^2}{2} g^{\mu\nu} \partial_\mu \theta \partial_\nu \theta - V(\theta) = -\frac{f^2}{2} g^{\mu\nu} \partial_\mu \theta \partial_\nu \theta - m_{\rm a}^2 f^2 (1 - \cos\theta).$

Neglecting fluctuations, the homogeneous zero-mode satisfies

$$\ddot{\Theta} + 3H\dot{\Theta} + m_{\rm a}^2(T)\sin(\Theta) = 0,$$

$H = \dot{a}/a$ = expansion rate of universe

(here a is the scale factor in the Friedmann-Roberston-Walker metric $ds^2 = dt^2 - a^2(t)\left[\frac{dr^2}{1-kr^2} + r^2 d\Omega^2\right]$!)

With initial conditions: $\Theta(t_i) = \Theta_i, \quad \dot{\Theta}(t_i) = 0.$ ***standard assumption***

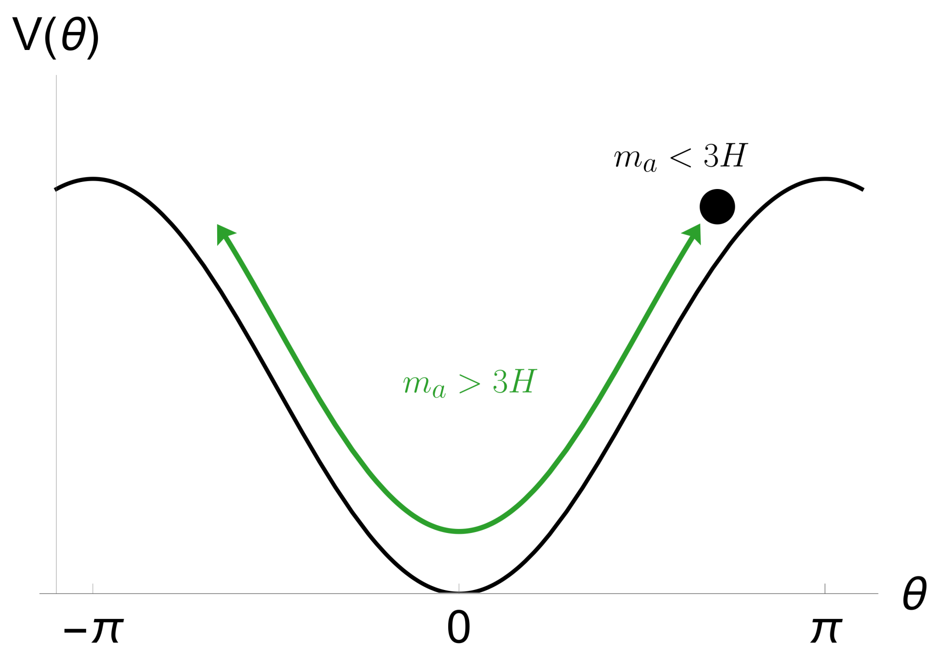

> $m_a \ll 3H \iff \rho_a \propto a^0$ (Frozen)

> $m_a \gg 3H \iff \rho_a \propto a^{-3}$ (Oscillating)

—> standard misalignment mechanism

For $\Theta_i \sim 1$ $\quad \rho_{\rm DM} \sim \rho_{osc} \left(\frac{a_{osc}}{a_0}\right)^3 \sim m_a^2 f_a^2 \left(\frac{T_0}{T_{osc}}\right)^3$

$$T_{osc} \sim \sqrt{m_a M_{Pl}}$$

ALP DM parameter space.

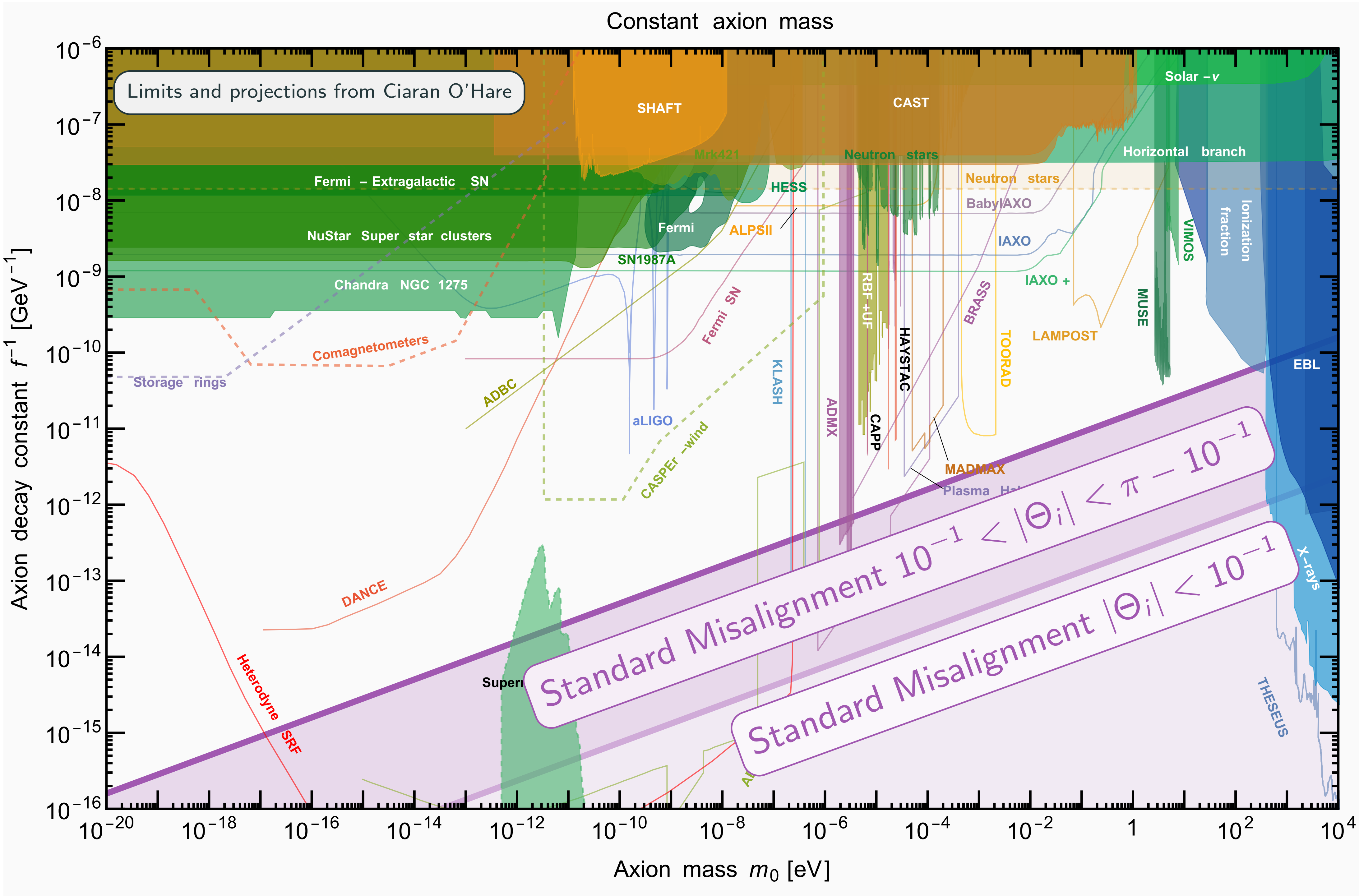

(KSVZ-like coupling)

$$g_{\theta\gamma} = (\alpha_{\mathbf{em}}/2\pi)(1.92/f))$$

Conventional misalignement makes too little DM for low f_a .

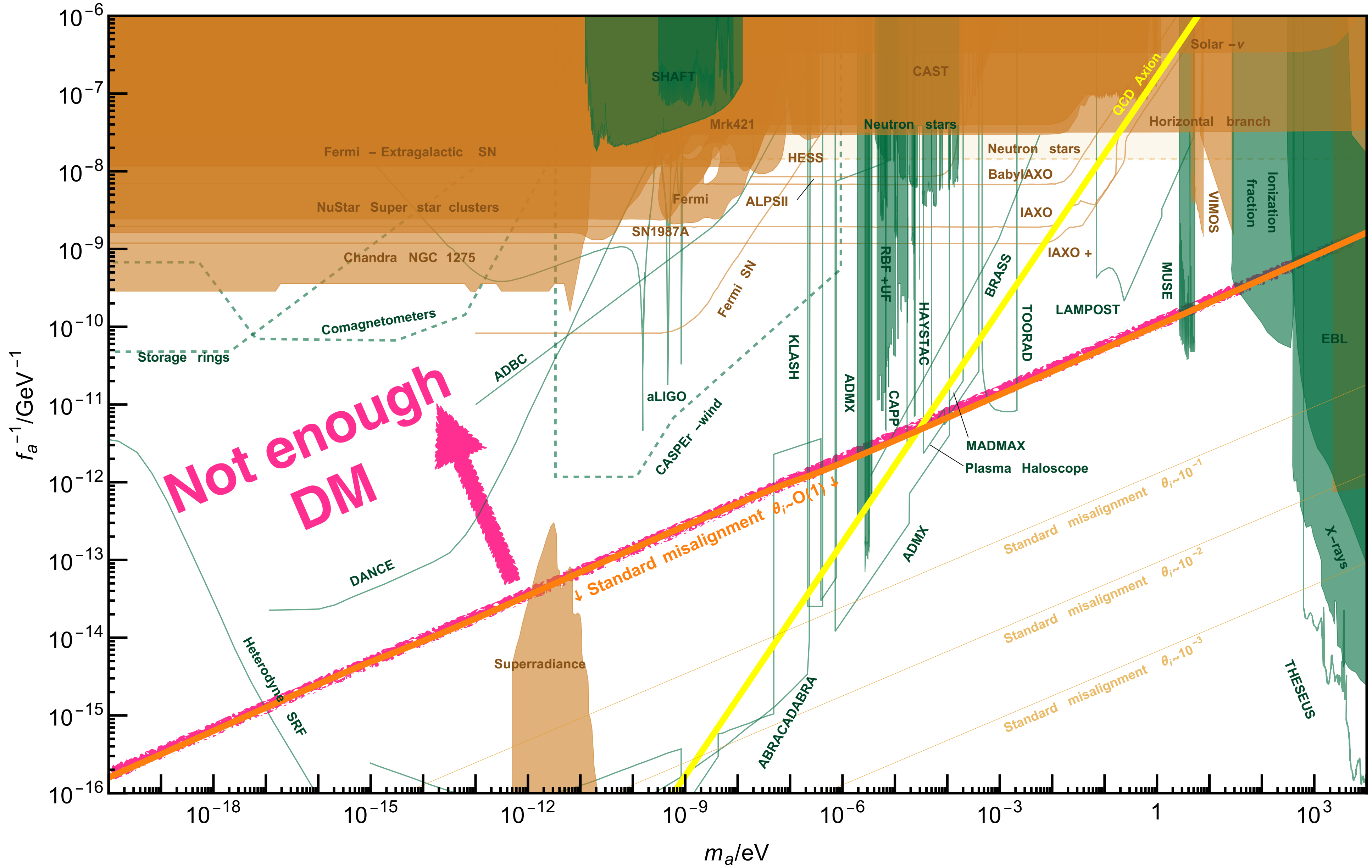

A way out: switch on initial velocity for the axion

Co, Harigaya et al ’19
Chang, Cui’19
Eroncel et al, ‘22